



NAVAL FACILITIES ENGINEERING SERVICE CENTER
Port Hueneme, California 93043-4328

Technical Report TR-2037-OCN

SEAWATER HYDRAULIC ROCK DRILL IMPACT MECHANISM MODEL VALIDATION

by

John P. Kunsemiller
and Bruce W. Farber

DTIC
ELECTE
MAR 14 1995
S G D

January 1995

Sponsored by
Office of Naval Research

19950308 216

REPORT DOCUMENTATION PAGE			Form Approved OMB No. 0704-018	
Public reporting burden for this collection of information is estimated to average 1 hour per response, including the time for reviewing instructions, searching existing data sources, gathering and maintaining the data needed, and completing and reviewing the collection of information. Send comments regarding this burden estimate or any other aspect of this collection information, including suggestions for reducing this burden, to Washington Headquarters Services, Directorate for Information and Reports, 1215 Jefferson Davis Highway, Suite 1204, Arlington, VA 22202-4302, and to the Office of Management and Budget, Paperwork Reduction Project (0704-0188), Washington, DC 20503.				
1. AGENCY USE ONLY (Leave blank)		2. REPORT DATE January 1995		3. REPORT TYPE AND DATES COVERED Final; Oct 1991 through Sep 1994
4. TITLE AND SUBTITLE SEAWATER HYDRAULIC ROCK DRILL IMPACT MECHANISM MODEL VALIDATION			5. FUNDING NUMBERS PR - RM33F61 WU - DN662005	
6. AUTHOR(S) John P. Kunsemiller and Bruce W. Farber				
7. PERFORMING ORGANIZATION NAME(S) AND ADDRESS(ES) Naval Facilities Engineering Service Center 560 Center Drive Port Hueneme, CA 93043-4328			8. PERFORMING ORGANIZATION REPORT NUMBER TR-2037-OCN	
9. SPONSORING/MONITORING AGENCY NAME(S) AND ADDRESSES Office of Naval Research 800 Quincy Street Arlington, VA 22217-5000			10. SPONSORING/MONITORING AGENCY REPORT NUMBER	
11. SUPPLEMENTARY NOTES				
12a. DISTRIBUTION/AVAILABILITY STATEMENT Approved for public release; distribution unlimited.			12b. DISTRIBUTION CODE UNCLASSIFIED	
13. ABSTRACT (Maximum 200 words) The Naval Facilities Engineering Service Center (NFESC) has developed and evaluated a computer model of the single poppet-kicker port linear impact mechanism used in the seawater hydraulic rock drill. The project objective was to identify hydraulic and dynamic elements influencing impact mechanism operation. A goal of this investigation was to determine whether or not computer modeling of the impact mechanism for the seawater hydraulic rock drill would lead to an improved linear impact mechanism suitable for a hand-held, diver-operated rock drill. Having achieved qualitative model response, the model served as an analysis tool for evaluating proposed changes toward achieving a minimum 7 foot-pound blow energy. Model parametric studies lead to validation of predicted performance improvements through hardware tests using the pre-production seawater rock drill with modified impact mechanism component parts. This document is the final report on a 3-year effort that has resulted in a better understanding of the hydraulic and dynamic elements influencing impact mechanism operation as well as a technique for analyzing complex fluid power components. At the conclusion of funding, the validated model showed a reliable 6 foot-pound blow energy. Additional development of the single poppet-kicker port linear impact mechanism is recommended using the validated model as a basis for optimizing the linear impact mechanism.				
14. SUBJECT TERMS Seawater, rock drill, tools, diver equipment, hydraulic equipment			15. NUMBER OF PAGES 45	
			16. PRICE CODE	
17. SECURITY CLASSIFICATION OF REPORT Unclassified	18. SECURITY CLASSIFICATION OF THIS PAGE Unclassified	19. SECURITY CLASSIFICATION OF ABSTRACT Unclassified	UL	

CONTENTS

	Page
INTRODUCTION	1
BACKGROUND	1
Requirements	2
Component Description	2
DYNAMIC MODEL	2
MODEL VALIDATION	3
Poppet Valve Coefficient	3
Minimized Drill Body Motion	4
Reductions to Plunger and Piston	5
Damping Coefficients	8
RESULTS	9
CONCLUSIONS	10
RECOMMENDATIONS	11
REFERENCES	12
APPENDIXES	
A - Details of DADS Model	A-1
B - Impact Mechanism Parts Drawings	B-1

Accession For	
NTIS	CRA&I <input checked="" type="checkbox"/>
DTIC	TAB <input type="checkbox"/>
Unannounced <input type="checkbox"/>	
Justification	
By	
Distribution /	
Availability Codes	
Dist	Avail and/or Special
A-1	

INTRODUCTION

Navy construction divers currently rely on oil hydraulic powered tools to perform various underwater construction tasks. In today's growing awareness for environmental responsibility, the Navy is actively pursuing technology that will minimize the risk of violating environmental regulations. One focus for technology development has been improved hydraulic tools for safe operation in and around environmentally protected waters. Commercial oil hydraulic powered tools can be replaced by intrinsically safe seawater hydraulic powered tools developed at the Naval Facilities Engineering Service Center (NFESC).

Seawater has proven to be an effective and environmentally safe substitute for hydraulic oil (Ref 1). The seawater hydraulic powered diver tool system, developed to satisfy the needs of the underwater construction diver, includes a bandsaw, rotary disk tool, and rotary impact tool. The system provides required capability without the hazards associated with using oil as the hydraulic fluid. The fourth construction tool developed for the system, a seawater hydraulic powered rock drill, has not been released because the linear impact mechanism was found to be unreliable and subject to unexplained variations in performance (Ref 2).

This task under the Navy Exploratory Development Technology Program Plan was funded through the Office of Naval Research in fiscal year 1992 with the objective of identifying the hydraulic and dynamic elements influencing impact mechanism operation. A goal of this investigation was to determine whether or not computer modeling of the impact mechanism for the seawater hydraulic rock drill would lead to an improved linear impact mechanism suitable for a hand-held, diver-operated rock drill. This document is the final report on a 3-year effort that has resulted in a better understanding of the single poppet-kicker port linear impact mechanism and a technique for analyzing complex fluid power components.

BACKGROUND

The seawater rock drill performance problem was attributed to the operation of the single poppet-kicker port linear impact mechanism. This mechanism provides cycle timing as well as impact energy to the drill operation. During testing of the original rock drill, small changes to component dimensions were found to produce wide variations in drill performance. The various influences on linear impact mechanism performance were not understood.

At the conclusion of the original seawater rock drill development, two recommendations were presented. The first recommendation was to investigate alternate impact mechanism designs in hopes of finding one more suited to development of a seawater hydraulic rock drill. The second recommendation was for independent development of the single poppet-kicker port linear impact mechanism. Computer modeling was recommended as a means to characterize performance through parametric studies without the need for expensive hardware fabrications (Ref 2).

The results of the computer modeling effort are documented in this report. The pursuit of the first recommendation lead to a separate parallel effort for the development and demonstration of a water hammer cycle impact mechanism. A successful Phase I proof of concept and an ongoing Phase II prototype demonstration water hammer drill have been funded

through the Small Business Innovative Research (SBIR) program. At the conclusion of the SBIR Phase II, the water hammer impact mechanism will be documented separately.

Requirements

The original design requirements for the seawater rock drill served as guidelines for this impact mechanism development. Drill performance was stated as having a penetration rate equivalent to the Stanley model HD-20 oil hydraulic hammer drill currently in the Underwater Construction Team (UCT) inventory. This was restated for our purpose as an impact mechanism capable of delivering to the drill steel and rock interface 7 foot-pounds of impact energy at a rate of 30 cycles per second. At this performance level with a 3/4-inch-diameter drill bit, a penetration of 3.5 inches per minute is calculated for rock having a 12,000 pounds per square inch compressive strength (Ref 3).

The prototype rock drill as-built weight was 49 pounds. Though 9 pounds heavier than the design requirement, it was previously agreed that the extra weight did not detract from drill operability. In the model, the drill weight was set at 50 pounds.

Component Description

The Pre-Production Prototype (3P) rock drill, shown in Figure 1, is configured with a single poppet-kicker port linear impact mechanism. The functional description of the cycle can best be understood by reviewing the diagram shown in Figure 2.

During tool operation, water at supply pressure enters the drill through the trigger valve and is directed into the drive chamber through the initially open supply poppet. This water flow in turn drives the plunger and the piston down into the drill steel creating a percussive impact at the rock surface. Near the end of the drive cycle, the relative position of the drive plunger within the plunger sleeve causes the kicker port to pressurize and closes the supply poppet. The closing of the supply poppet results in a bleed down of drive chamber pressure allowing the piston return to reset the plunger. During plunger reset, the relative position of the drive plunger within the plunger sleeve relieves the kicker port and permits the supply poppet to open. From this point the cycle repeats.

Exhaust flow from the linear impact mechanism is directed to the 3-horsepower seawater motor to index the drill steel. Motor exhaust is discharged to ambient out the motor exhaust port.

DYNAMIC MODEL

The software selected for model development was the Dynamic Analysis and Design System (DADS). The developed computer model of the linear impact mechanism qualitatively mimicked empirical test results obtained during prior rock drill evaluation testing. After model validation, parametric studies were performed for comparison to baseline model results. Model refinements lead to predictions of performance improvements. These improvements were validated using the 3P drill to test modified impact mechanism component parts.

The basic building blocks for the model consisted of bodies, some fixed to an inertial reference frame, and some allowed to move; joints between the bodies; springs; hydraulic

accumulators; valves; actuators; line elements; and control functions. Figure 3 shows the basic hardware components.

The control and hydraulic functions in the model were divided into four sections:

- 1 - Supply Pressure Activation
- 2 - Poppet Motion
- 3 - Plunger Motion
- 4 - Piston Motion

Detailed descriptions of each section are provided in Appendix A.

MODEL VALIDATION

Parametric studies were conducted using the computer model as a tool to optimize linear impact mechanism performance. Model features were added or adjusted to simulate changes to the linear impact mechanism design. Drill hardware testing validated predicted model results. Since some of the model parameters were approximated rather than measured values, a precise matching of the results was not expected nor necessarily desired. The focus of the effort was to evaluate model trends and relate findings to specific hardware parameters. The first finding dealt with the sensitivity of the model to small changes in supply poppet valve flow coefficient.

Poppet Valve Coefficient

As reported in Reference 2, the shape of the supply poppet seat affected drill operation. It was empirically found that a grooved valve seat produced desirable results. This annular groove had the effect of increasing the valve's flow coefficient. The model showed weak impacting from low piston velocities with smaller valve flow coefficients. Conversely, greater impact energies from high piston velocities were modeled using larger valve flow coefficients.

An experiment was conducted to quantify the differences in behavior between the grooved and the nongrooved poppet. It was also an objective to determine the validity of the valve coefficient used in the model. Steady flow and dynamic flow conditions were evaluated. Figure 4 is a schematic of the test fixture.

During the static tests, the displacement of the poppet was fixed either full open or nearly closed. The pressure drop across the valve was measured for several flow rates. The valve flow coefficient obtained for the grooved and nongrooved poppet are shown in the graph of Figure 5.

No significant difference between poppets was observed for a nominal displacement of 0.050 inches. The value of the open poppet flow coefficient was close to the modeled value of 5. The smooth poppet yielded a higher valve flow coefficient for a nominal displacement of 0.015 inches. This was opposite of what was expected and has not been explained. The curves also show that as the valve opens, the grooved poppet flow coefficient increases, whereas the smooth poppet flow coefficient decreases.

During dynamic tests, poppet valve configurations for grooved and nongrooved poppets were evaluated with and without the biasing spring. Evaluation of one open-close cycle was representative of valve operation, however, manual control of the flow to the kicker port limited

cycle speed. Figure 6 presents two graphs comparing dynamic cycle test results for grooved and nongrooved poppet seats, both with the biasing spring.

There did not appear to be any significant difference between the behaviors of the grooved and nongrooved poppets. As in the static tests, the expected differences between the grooved and nongrooved poppets was not substantiated.

One series of model runs focused on changing the area values in the poppet actuator elements to cause the poppet to open more quickly. In the model, the desired effect was achieved by increasing the opening area from 0.0182 square inches to 0.0382 square inches and decreasing the closing area from 0.1329 square inches to 0.1129 square inches. The improvement was small and suggests that enlarging the poppet area is not detrimental to impact mechanism performance. Later, drill hardware tests showed equal results when using the nongrooved poppet suggesting that the grooved feature is not required.

Minimized Drill Body Motion

Movement of the drill body was identified early in the evaluation process as a key influence on impact mechanism performance. The impact mechanism optimization process, therefore, used drill body displacement as a measure of cycle performance. During cycling of the impact mechanism, hydraulic pressure driving the plunger and piston downward also lifts the drill body up. The concern is the movement of the plunger sleeve in the drill body and the relative position of the sleeve with respect to the plunger during the cycle. There is a point where the drill/sleeve has moved far enough up from nominal such that the kicker port is actuated before piston impact against the anvil. The result is a missed or weak impact caused by the premature actuation of the kicker port to close off drive chamber supply.

Hardware testing was performed using a test stand that held the drill upright and allowed the drill unrestricted vertical displacement. A force transducer was used to measure impact force. This transducer was calibrated by dropping a 10-pound weight from 1 foot to obtain a measurement for 10 foot-pounds of potential energy. A Temposonic position transducer measured the vertical displacement of the drill body. One accelerometer was attached to the drill body and a second to the impact plate at the base of the test stand. The accelerometers did not provide useful data, since they were somewhat noisy. The measurements using the force transducer and Temposonic transducer provided repeatable data.

The drill was modeled at the operating condition of 1,500 psi supply pressure with a 50-pound force applied as the weight of the drill. This model showed a drill body displacement of over 0.4 inches. Hardware testing confirmed a smaller 0.12-inch drill body displacement and showed a qualitative improvement in drill cycle rate with the application of downward force to the drill. This confirmed the relation between drill body movement and impact mechanism performance.

Two methods were applied to minimize drill body motion. The approach was to first optimize operating pressure for the existing drill weight of 50 pounds. Reduced operating pressure resulted in less energy to the tool to cause drill body movement. This is evident in the model results shown in Figure 7 obtained with an additional 150-pound downward force applied. Best drill performance was selected at 1,000-psi system pressure.

Then, additional downward force representing increased drill weight was added until consistent energy transfer was achieved. Adding 100 pounds downward force in the model was insufficient for reducing drill body displacement while 150 pounds downward force reduced drill body displacement by a factor of two. Adding 200 pounds or 400 pounds downward force

nearly eliminated drill body displacement. In all cases, the cycle repeatability in terms of magnitude and repetition of impacts improved with an increase in applied downward force. Figure 8 shows drill body displacement reductions for several values of added force.

Reductions to Plunger and Piston

From a practical standpoint, a 150-pound or more rock drill was not an acceptable solution. What was desired was an optimized impact mechanism for the 50-pound drill weight. Viewed as an energy balance problem, improvement was expected through a scaled reduction of the plunger and piston size. The energy used to drive the scaled plunger and piston produced less reaction force to displace the rock drill body.

Table 1 shows a comparison of several parameters used in the baseline 3P drill with those tested as part of the validation of the reduced plunger and piston areas. Drawings of the redesigned plunger, plunger sleeve, sleeve cap, and piston are provided in Appendix B.

Of several model runs at various values of plunger and piston areas, the best results were produced with a plunger area reduction of 30 percent and a piston return area reduction of 36 percent. The ratio of plunger area to piston return area has a measurable effect on cycle timing. Some slowing of the cycle was desired to preserve timing functions. This necessitated the 6 percent greater reduction in piston return area. Further investigation into timing effects revealed that by opening the kicker port to the exhaust port sooner (i.e., move the kicker port closer to the exhaust port in the plunger sleeve), the amount of external applied force could be reduced to 100 pounds.

Table 1
Comparison of Evaluated Design Parameters

Parameter	Baseline Production Drill	Redesign Validation
Operating Pressure	1,500 psi	Tested at 600, 1,000, and 1,500 psi
Added Weight	0	Tested at 0 and 100 lb
Plunger Head Diameter/ Area	0.555 in. 0.24 in. ²	0.466 in. 0.17 in. ²
End Cap on Plunger	Yes	No, single diameter
Plunger Stop (lower)	Sleeve	Piston
Plunger Length	3.687 in.	3.996 in.
Piston Return Area	0.0807 in. ²	0.0514 in. ²
Groove in Poppet	Yes	No
Piston Stop (upper)	Housing	0.31 in. down

The decrease in plunger area from 0.24 square inch to 0.17 square inch was accomplished with a plunger of the smaller diameter without an end cap feature. The plunger mass and travel limits were adjusted in the model to represent this redesign. The single diameter plunger traveled in contact with the piston throughout the piston stroke. To maintain cycle timing at the lower end of the stroke, the plunger length was extended 0.31 inch to position the plunger cutout between the kicker port and the supply pressure port. This plunger configuration eliminated the "dead band" in piston stroke inherent in the 3P drill. The portion of the piston stroke in the 3P drill where the plunger is no longer in contact and driving the piston is referred to as the "dead band" portion of the piston stroke. The dead band occurred when the plunger came to rest in the sleeve at the stop for the end cap. During this portion of the stroke, the piston undergoes deceleration caused by piston seal friction and by a continuously energized piston return. Eliminating the dead band by driving the piston continuously to anvil impact improved impact mechanism efficiency.

A reduced upper piston diameter provided a net piston return area of 0.0514 square inches giving a piston return force of 51 pounds at 1,000-psi supply pressure. The piston mass was adjusted to represent the change. A spacer was added to the top of the piston sleeve to prevent over stroking the lengthened plunger. This spacer did not decrease the operating stroke of the impact mechanism as the stroke length is bound by the timing of the kicker port actuation. The piston hard stop was modified to reflect the new location between the piston housing and the top of the piston.

Referring to Table 2, testing of the baseline impact mechanism using the 3P drill parts produced the results shown as Tests 1, 2, and 3 (direct measurement of body motion was not available for these tests). The data showed erratic impacts and wide variability. No weight was added to the drill for the first test set. The results of the baseline model, adjusted to match the configuration of Test 1, are included in the lower portion of the table. The data for all 1,000-psi supply pressure sets is in bold typeface for comparison.

A comparison of individual data for Tests 1 through 3 shows a large spread in the range of impact energy. A closer review of the test data indicates a pattern of short cycling producing inconsistent impact energy. Comparing Test 1 to the baseline model shows general agreement in cycle time but the model predicted larger impacts with less variation. The addition of 100 pounds in the model had the expected increase in impact energy but also increased the variability of the data.

Tests 4, 5, 6 were conducted with the 36 percent reduced area piston installed. This resulted in longer cycle times and an order of magnitude less drill body displacement than predicted by the baseline model. Tests at 1,000- and 1,500-psi pressures showed a double impact with the second impact being far smaller than the first. The reason for the double impact is discussed in the next section on damping coefficients. It is clear, however, that the double impacts are responsible for the unexpected longer cycle times at the higher pressures. An example of this double impact is shown in Figure 9 for the Test 5 data.

Table 3 presents the results from seven tests conducted with the 30 percent reduced plunger and 36 percent reduced piston installed. For Test A2 and Test A7, a test operator leaned full weight on the drill, applying an estimated 100 pounds of force downward on the drill. The baseline model was updated to match the configuration of Test A2. The redesign model results are displayed in the lower half of Table 3. The data for all 1,000-psi supply pressure sets is in bold typeface for comparison.

Table 2
Comparison of Baseline Test Results

Test No.	Pressure (psi)	Added Weight (lb)	Cycle Length (ms)	Impact Energy Range (ft-lb)	Body Motion (in.)
1	600	0	40	0.06 to 0.12	N/A
2	1,000	0	27	0.7 to 2.2	N/A
3	1,500	0	25	0.9 to 3.9	N/A
4	600	0	40	0.4 to 0.7	0.01
5	1,000	0	50	3 to 3.8	0.03
6	1,500	0	70	4.5 to 4.8	0.05
Baseline Model	1,000	0	31	1.3 to 2.5	0.4
Baseline Model	1,000	100	31	1.5 to 4.5	0.4

Table 3
Comparison of Redesign Test Results

Test No.	Pressure (psi)	Added Weight (lb)	Cycle Length (ms)	Impact Energy Range (ft-lb)	Body Motion (in.)
A1	1,000	0	27	1 to 2.6	0.05
A2	1,000	100	24	1.2 to 3	0.01
A3	600	0	35	first: 0.7 0.2 to 0.5	0.01
A4	1,500	0	19	1.2 to 2.7	0.25
A5	1,500	0	19	first: 4.4 0.7 to 2	0.1, 0.01
A6	1,350	0	20	first: 5 0.7 to 1.6	0.1, 0.01
A7	1,500	100	20	2.5 to 7	0.03
Redesign Model	1,000	100	19	2.3 to 3.3	0.27

Comparing Table 3 data to Table 2 data, we find for baseline Test 2 and redesign Test A1, both with no weight added, the impact energy increased a small amount presumably from reduced drill body displacement. This was also the case for Test 1 and Test A3. This seems to validate model prediction. However, this does not hold true when comparing Test 3 to Tests A4 or A5. It appears that the shorter cycle length in the later tests contributed to reduced impact energy.

During data collection for Tests A5 and A6, the drill was observed to operate in two modes. The first mode showed an initial displacement of the drill body, and then resulted in a fast cycle with low force impacts about that displacement. The second mode caused the drill body to rise and fall at low frequency with higher impact force. The pressure from the supply also dropped slightly during the second mode operation indicating an increase in flow rate. During Tests A3, A5, and A6, the initial impact was far higher than subsequent impacts suggesting that the initial impact had a direct effect on mode selection and that Test A3 may also have been a first mode operation. Figure 10 shows the drill body displacement and impact energy for this condition.

Test A7 results are for the drill operating in the second mode with approximately 100 pounds applied to the drill. The larger amplitude force impacts tracked with drill displacement. When the drill body displacement was small, the impact strength was greatest. This confirmed model predictions for minimizing drill body displacement to maximize impacts. Figure 11 shows, for Test A7, nearly half of the impacts were at 6 foot-pounds or greater, though there was still a large spread in the range for impact energy.

At 1,000-psi operating pressure and with 100 pounds weight added to the drill, the redesign model showed slightly higher impact energy (2.3 to 3.3 foot-pounds versus 1.2 to 3 foot-pounds), significantly greater drill body motion (0.27 inches versus 0.01 inches), and shorter cycle time (19 ms versus 24 ms). However, when compared with test results from Test A4, run at 1,500 psi with no added weight, the cycle time and body motion of the redesigned model match more closely.

Damping Coefficients

The model behavior relating impact energy to added weight/reduced drill body displacement was evident in the hardware tests; however, model behavior seemed to correlate better with results from higher pressure test conditions. Inconsistent cycling in the redesign model and in hardware tests continued to thwart an exact comparison. An analysis of model parameter for the damping coefficients was conducted to further validate the model to test conditions.

With the longer plunger remaining in contact with the piston until impact with the anvil, the plunger cutout does not dwell in the "open" position (energizing the kicker port from the supply port). In the baseline drill, the plunger stopped in a position that allowed sufficient time to fully energize the kicker port. When the kicker port is not fully energized, the poppet does not close leaving the plunger chamber pressurized for a secondary impact. This "double impact" occurs with much less energy than the primary impact. Sometimes, a tertiary impact with even less energy than the secondary impact may occur before a new cycle can begin.

Test results exhibited suspected "double-impact" events at higher operating pressures (e.g., Test 6 at 1,500 psi). It was determined that insufficient damping was included in the hard stops, which explained why double impacting occurred in the DADS model at a lower operating pressure than in the test results. In the redesign model, a uniform value of 2.5 lb (in./sec) was used for damping. This corresponded to a range of 8 to 28 percent of critical damping

depending on the element. The damping in each hard stop was changed individually to a value representing 38 percent of critical damping (corresponding to a coefficient of restitution of 0.3, a typical value for metal-to-metal contact). The redesign model was adjusted for increased damping coefficients, with the results shown in Table 4.

Table 4
Comparison of Adjusted Model Results
[Pressure = 1,000 psi, Added Weight = 100 lb]

Test	Cycle Length (ms)	Impact Energy Range (ft-lb)	Body Motion (in.)
Test A2	24	1.2 to 3.0	0.01
Redesign Model	19	2.3 to 3.3	0.27
38% Damping Model	25	1.2	0.004
30% Damping Model	25	1.4	0.007

Increased damping produced an order of magnitude reduction in predicted drill body displacement matching test data under similar conditions. The model predicts a more regular impact energy with little spread in the value. As expected, there was a corresponding decrease in the impact energy for the model. Compared to Test A2, the 38 percent damping model yielded an increased cycle length to slightly longer than that in the test data (25 ms versus 24 ms), but a decreased impact energy to the bottom of the test data range (1.2 foot-pounds versus 1.2 to 3 foot-pounds). A small reduction to the damping coefficients (30 percent of critical damping) increased both the impact energy and body motion to values closer to those measured in Test A2. Figure 12 presents the impact energy, body motion, and piston stroke relative motion plots, respectively, for the model with the 30 percent damping coefficients.

RESULTS

A common occurrence during model development was the discovery of several variables that influenced an observed parameter of impact mechanism performance. One such variable involved the length of the plunger cutout which was known to control cycle timing. While adjustment of the damping coefficients eliminated the double impact, the model showed that lengthening the plunger cutout from 0.75 inches to 0.95 inches also eliminated the double impact phenomenon even for higher pressures and impact energies. Though appropriate correction of the damping coefficients achieved the desired effect, it is worth noting the possibility that impact mechanism sensitivity to one variable may be reduced by smaller adjustments to several variables.

In several model experiments, the ratio of plunger area to piston return area proved to be an important variable for achieving stronger impacts. In the first example, the model showed that for a 58 percent decrease in the piston return area, to 0.0340 square inches, the impact energy increased by approximately 40 percent in comparison to the increased damping coefficient model results. Since further reduction in piston return area was not desirable, the ratio was adjusted by an increase in the plunger area.

In a model experiment, the plunger area was doubled to 0.34 square inches. The drill cycled evenly, with impact energies averaging 6 foot-pounds (this was close to the desired result of 7 foot-pounds). Despite the larger plunger area causing larger actuator forces, the drill body displacement was less than 0.15 inch and there were no short cycles or missed impacts. The shape of the plunger/piston motion curve has a sawtooth shape, with a long return run, allowing gravity to act on the drill body to slow its upward speed and begin to return it to its starting position. Each subsequent drive stroke imparted an upward displacement, but gravity mitigated drill body displacement during a longer cycle time of 40 ms, or 1,500 beats per minute. Figure 13 shows the impact energy, body motion, and piston stroke relative motion plots for the model with the doubled plunger area.

Finally, hardware tests showed the impact mechanism to be sensitive to flow restriction at the exhaust orifice. When the rotary drive motor was connected to the circuit in series to the impact mechanism, the impact cycles became erratic and the number of cycles per second decreased. An externally applied force to the drill caused the rotary motor to stall, causing the impact cycle to become irregular or stop.

Because the stalled motor increases the back pressure at the exhaust orifice, flow through the impact mechanism is reduced to the point where the pressure across the impact mechanism is insufficient to produce a cycle. A pressure relief valve installed on the motor supply line and set to 350 psi produced no change in behavior. When the relief valve was set at 50 psi, the impact cycles became more regular. In this condition, an externally applied force stalled the motor but had no affect on cycle performance. Intermediate pressure settings produced a corresponding reduction in cycle performance.

CONCLUSIONS

The following conclusions are presented as a summary of the development and validation process for the computer model of the linear impact mechanism used in the seawater hydraulic rock drill:

1. The computer model of the single poppet-kicker port linear impact mechanism has been validated for both the baseline (using production parts), and the redesign rock drills. The damping coefficients, bulk modulus, and other model parameter values have been determined such that the model results closely match the test data for cycle time, body motion, and impact energy. The validated model shows a reliable 6 foot-pound blow energy, just short of the required 7 foot-pound level necessary for the rock drill design.

2. The linear impact mechanism model provides a cost effective tool for evaluating design modifications. The predictions of drill performance for an applied force, a reduced supply pressure, a change in poppet area, and a reduced plunger and piston size were experimentally verified. The pressure and motion curves predicted by the model matched the

empirical behavior well. The use of the Dynamic Analysis and Design System (DADS) software and the modeling techniques developed under this tasking has extended the Navy's capability to design complex seawater hydraulic system components.

3. The model predicts a small improvement in impact mechanism performance from an increase in the supply poppet valve size. Validation testing confirmed that the groove in the seat of the supply poppet valve is not necessary. Elimination of the grooved feature from the production drill and substitution of a larger valve seat can reduce component cost.

4. The seawater motor, presently plumbed in series with the impact mechanism, produces unacceptable back pressure variations to the impact mechanism resulting in erratic behavior and poor impact mechanism performance. Model results confirm that the motor supply must be decoupled from the linear impact mechanism drive chamber pressure if the impact mechanism is to cycle properly.

5. The smaller, single diameter plunger resulted in a significant reduction in impact energy with a corresponding reduction in drill body motion. Extending plunger length and eliminating the dead band portion of the piston stroke improved impact mechanism efficiency. Use of a single diameter plunger and plunger sleeve can reduce component fabrication cost while improving impact mechanism performance.

6. The cause of the two distinct modes of drill body motion observed during drill operation has not been identified. Impact mechanism performance continues to show dependence on drill body motion. Test results confirm that minimizing drill body displacement is necessary to maximize impact mechanism performance. Reducing the supply pressure, increasing the applied force on the drill body, and changing the cycle timing have made demonstrable improvements to impact mechanism performance because of small drill body displacement.

7. The model predicts impact energy values close to the design goal of 7 foot-pounds for a plunger area of 0.34 square inches. The oversize plunger produced a slow return stroke and maintained the drill body position within 0.15 inches. This allowed consistent impact energy. Further improvements were predicted by the model for a lengthened plunger cutout which successfully prevented double impacting, without decreasing impact energy.

RECOMMENDATIONS

A goal of this effort was to produce design data for a linear impact mechanism that could be transitioned into a usable diver-operated rock drill. Complete realization of this goal has not been attained. The single poppet-kicker port impact mechanism has proven to be a complex mechanism. There is still much that is not understood such as the observed dual mode drill body displacement behavior. The validated model now serves as a tool that can be used in the optimization process to reach the design requirement of 7 foot-pounds impact energy. Because it is more cost effective to conduct the optimization process using the validated computer model, further optimization of the impact mechanism model is recommended prior to any hardware testing. The following recommendations, based on observed model results, should provide the basis for achieving the design requirement:

1. The relationship between plunger and piston areas should be fully explored. Model experiments are recommended to determine the best values for plunger and piston sizes that will produce more than 7 foot-pounds on a consistent basis, without increasing drill body motion. Model results should be confirmed through testing of modified impact mechanism component parts.

2. The lengthened plunger cutout should be experimentally evaluated as a means to eliminate double impacting in combination with any future design seeking higher impact energies.

3. The seawater drive motor for bit indexing and related elements should be added to the DADS model to determine what parameters can be altered to compensate for the observed negative effects on hardware performance. The effects of adding the seawater motor in parallel and in series to the linear impact mechanism should be compared for selection of the best drill performance.

4. Finally, the Dynamic Analysis and Design System (DADS) software and the modeling techniques developed under this tasking should be applied to the design of complex seawater hydraulic system components. Use of this capability will enhance component performance and result in significant cost savings over traditional build and test methods of hardware development.

REFERENCES

1. J. Kunsemiller and S. Black. "Case study of an environmentally safe diver tool system", presented at the Underwater Intervention Conference, San Diego, CA, Feb 1994.
2. Naval Civil Engineering Laboratory. Technical Note N-1826: Development of a seawater hydraulic rock drill, by J. Kunsemiller. Port Hueneme, CA, Mar 1991.
3. William C. Maurer. Advanced drilling techniques, Chapter 2. Tulsa, OK, Petroleum Publishing Co., 1980.

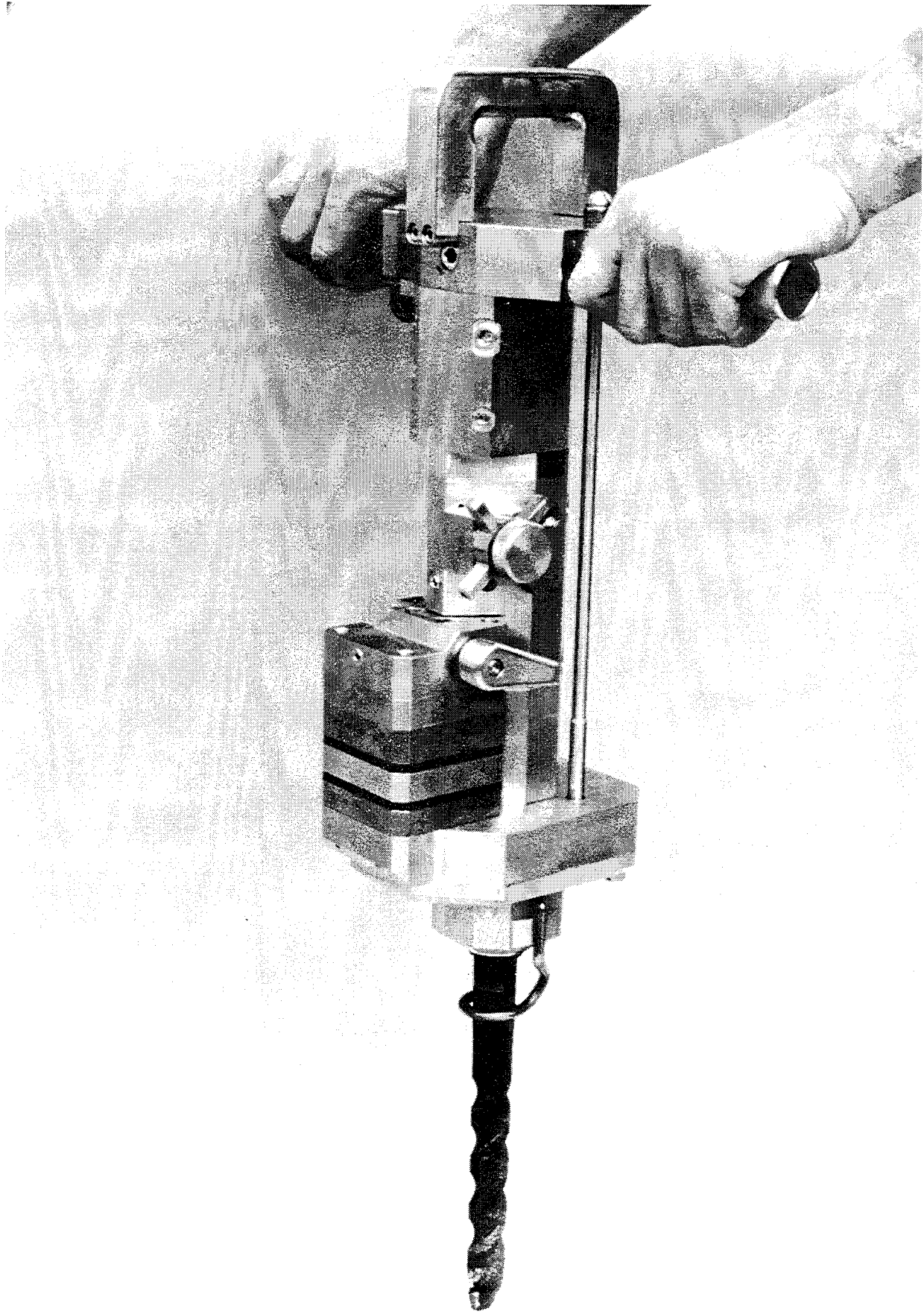


Figure 1
Pre-Production Prototype (3P) rock drill.

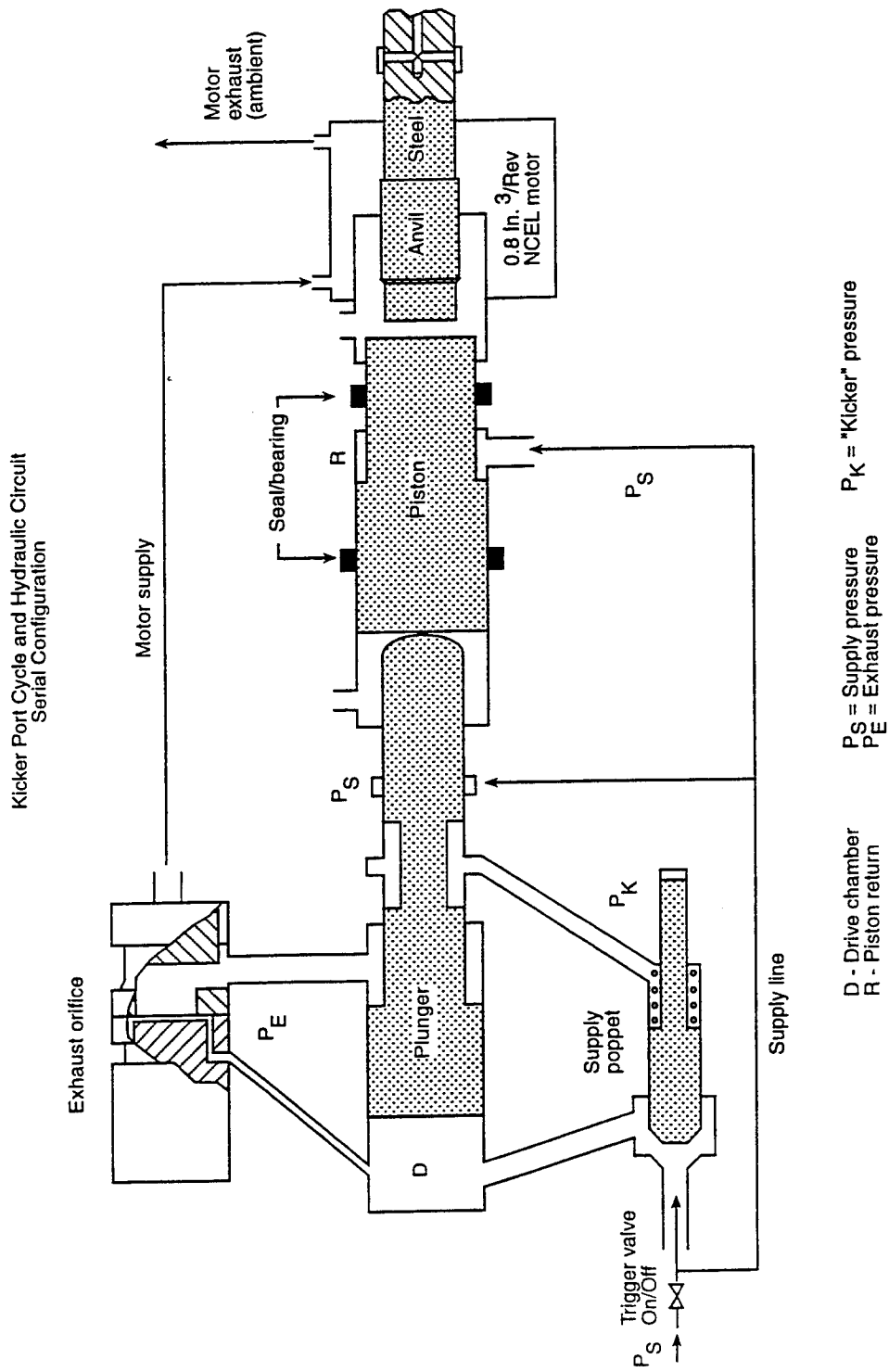


Figure 2
3P rock drill single poppet-kicker port linear impact mechanism diagram.

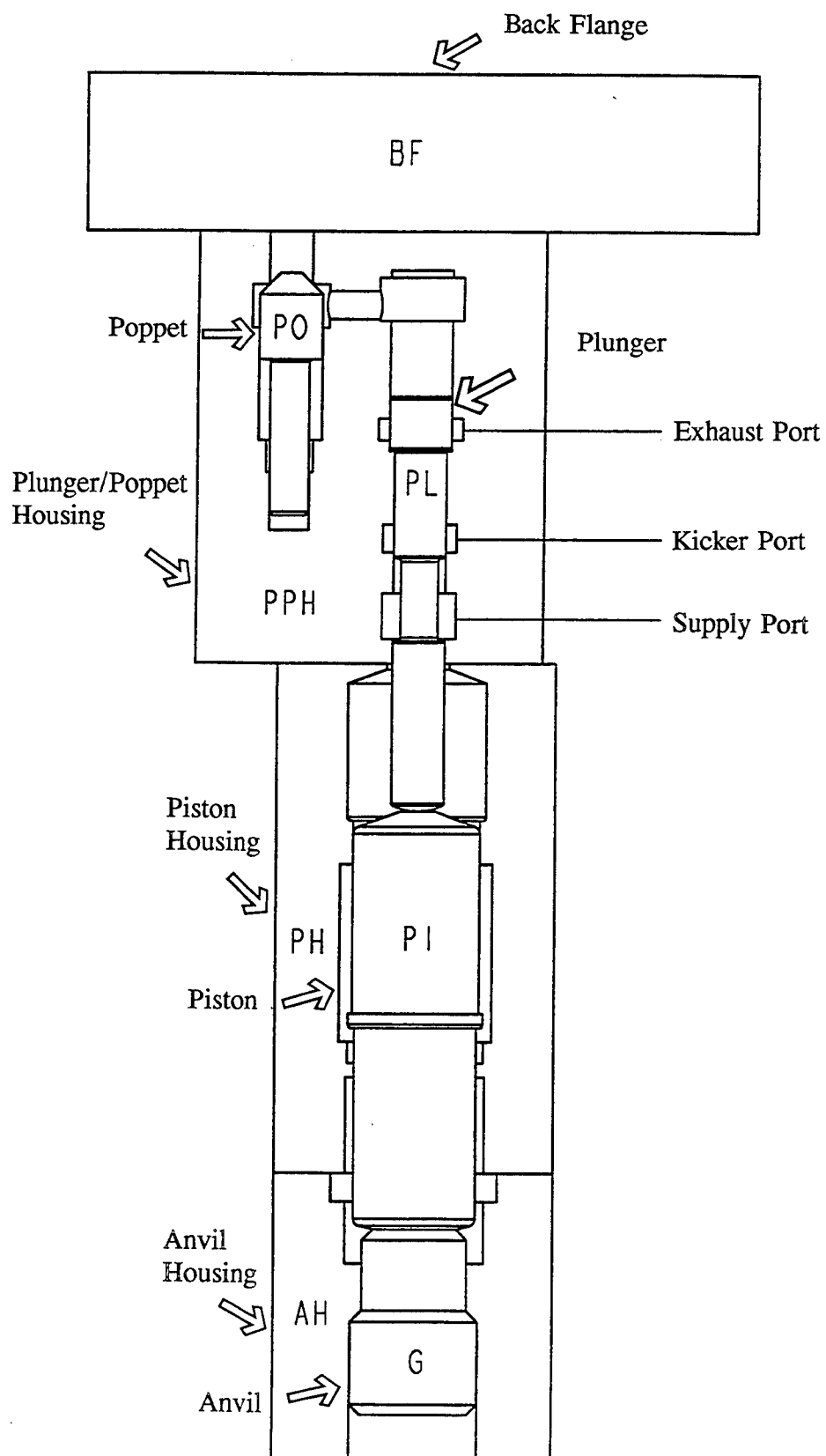


Figure 3
Basic model hardware components.

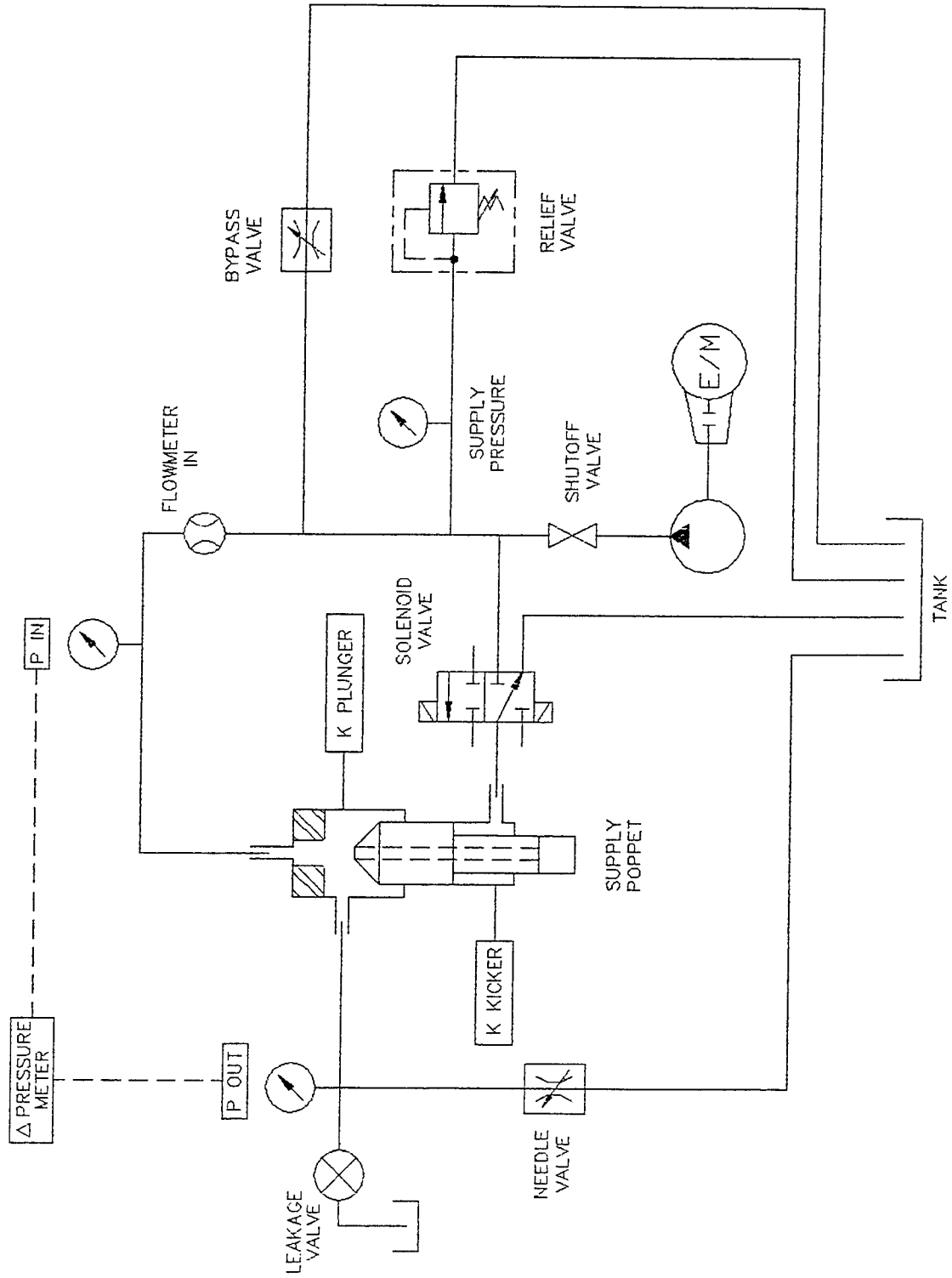


Figure 4
Flow coefficient test schematic.

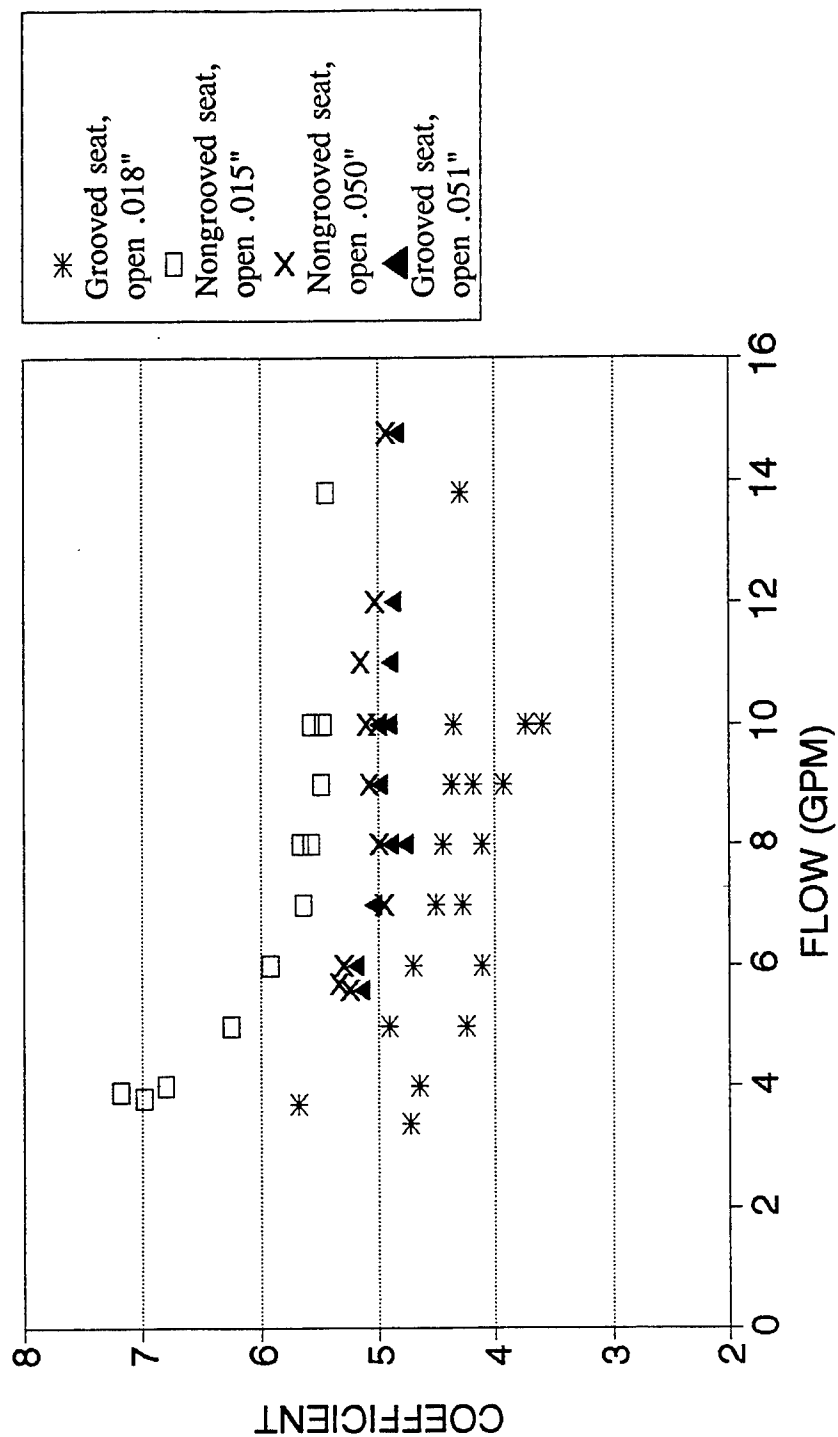
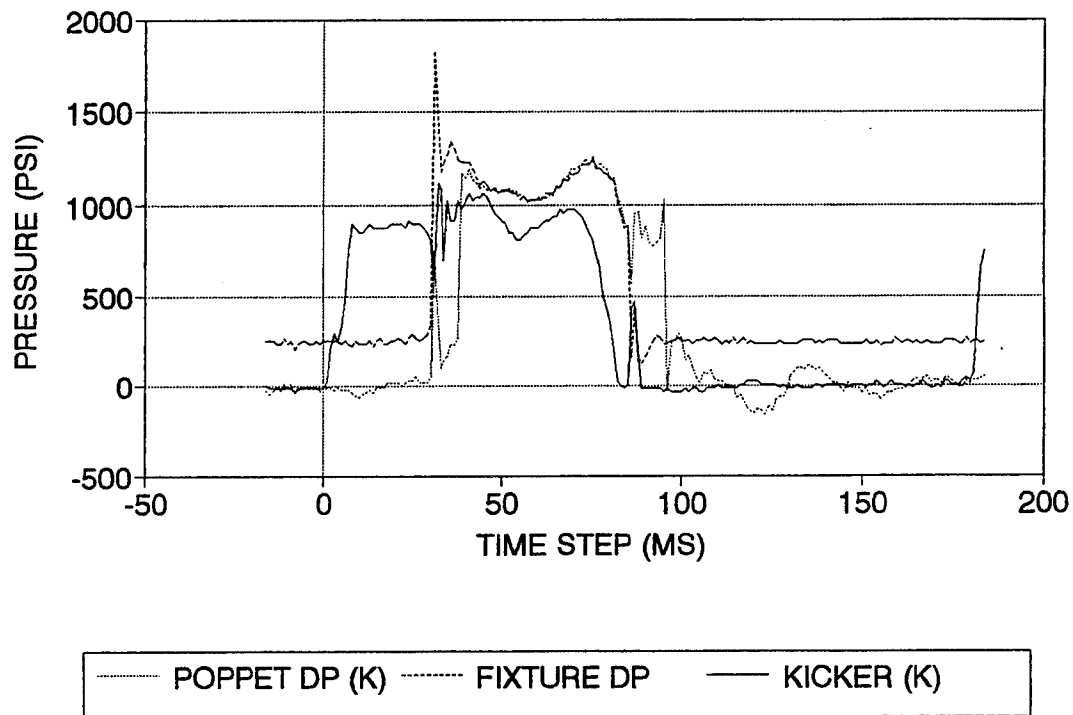
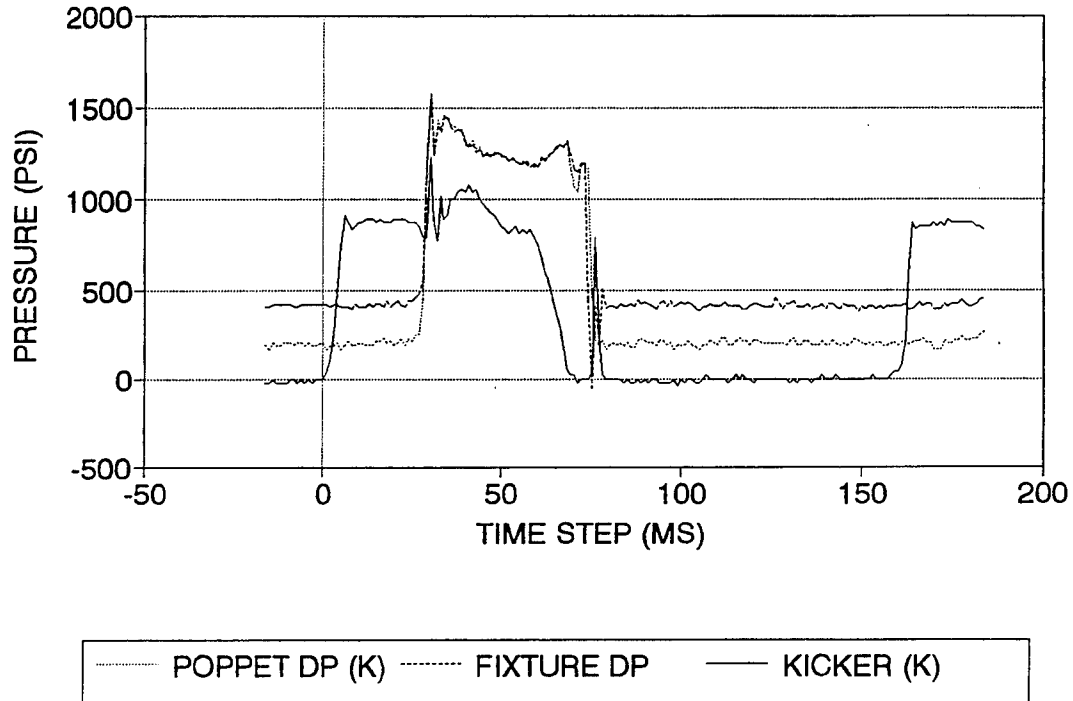


Figure 5
Graph of static flow coefficients for grooved and nongrooved poppet seats.



(a) Cycling - grooved poppet, with spring.



(b) Cycling - smooth poppet, with spring.

Figure 6
Graph of dynamic test for grooved and nongrooved poppet seat.

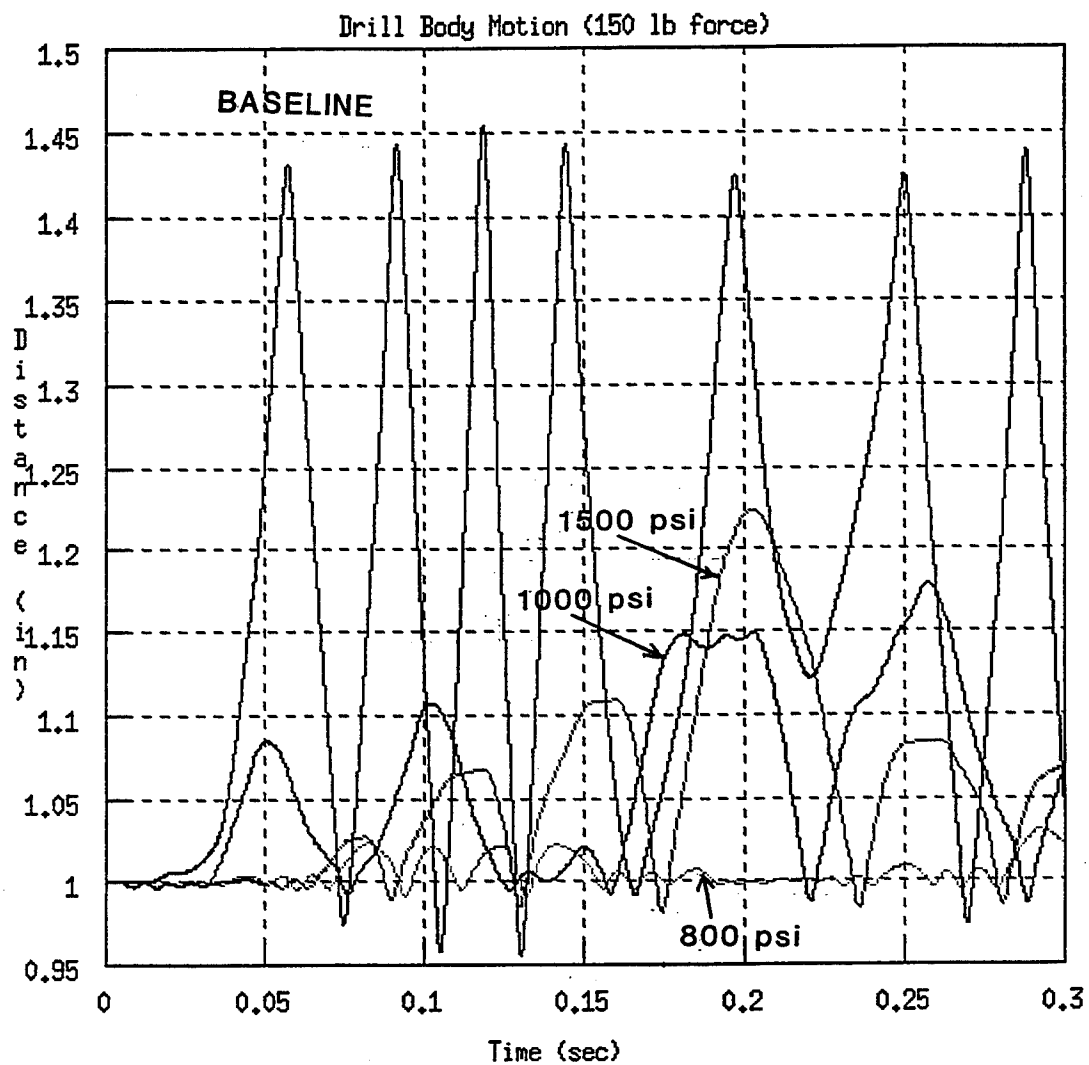


Figure 7
Comparison of drill body displacement for pressures from 800 to 1,500 psi.

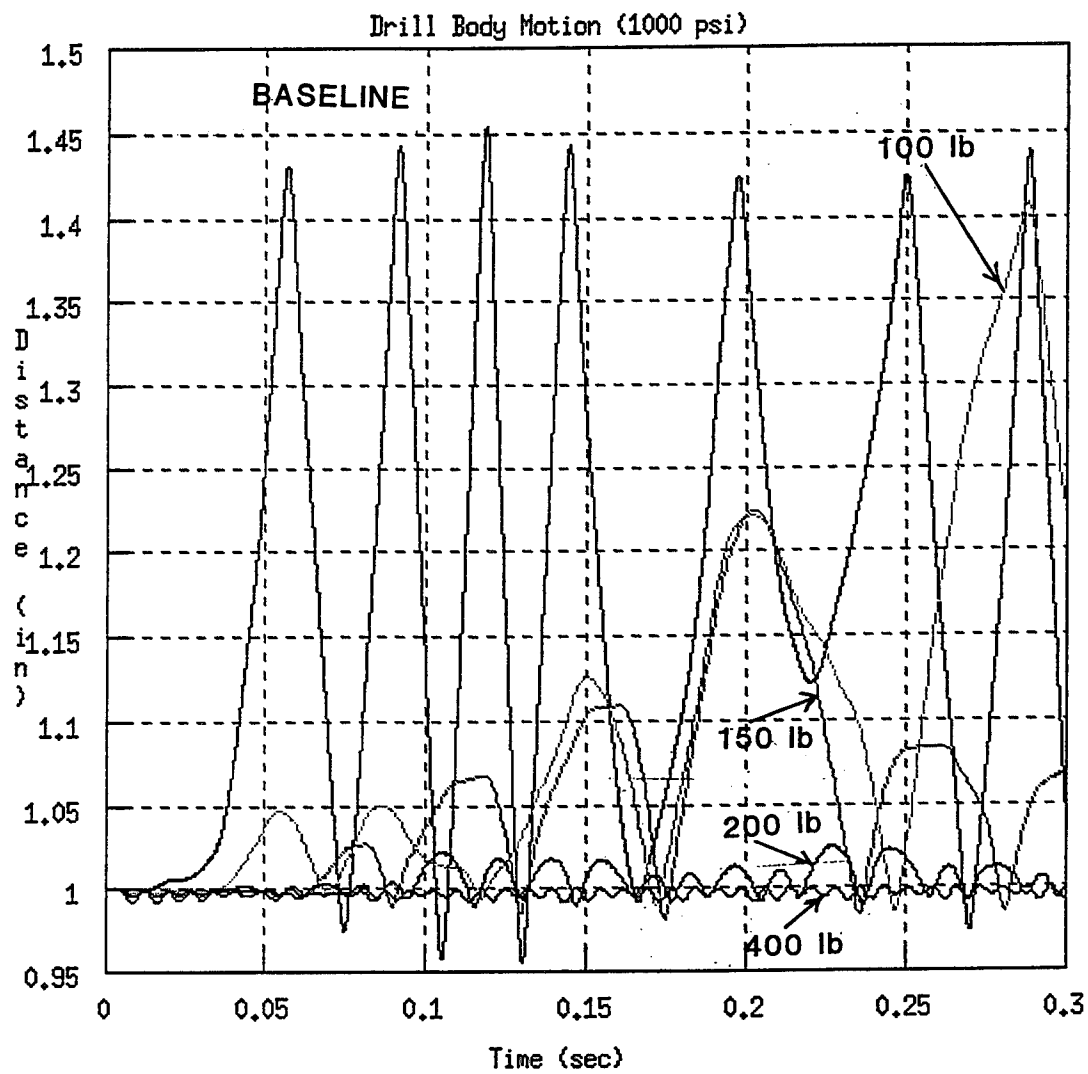
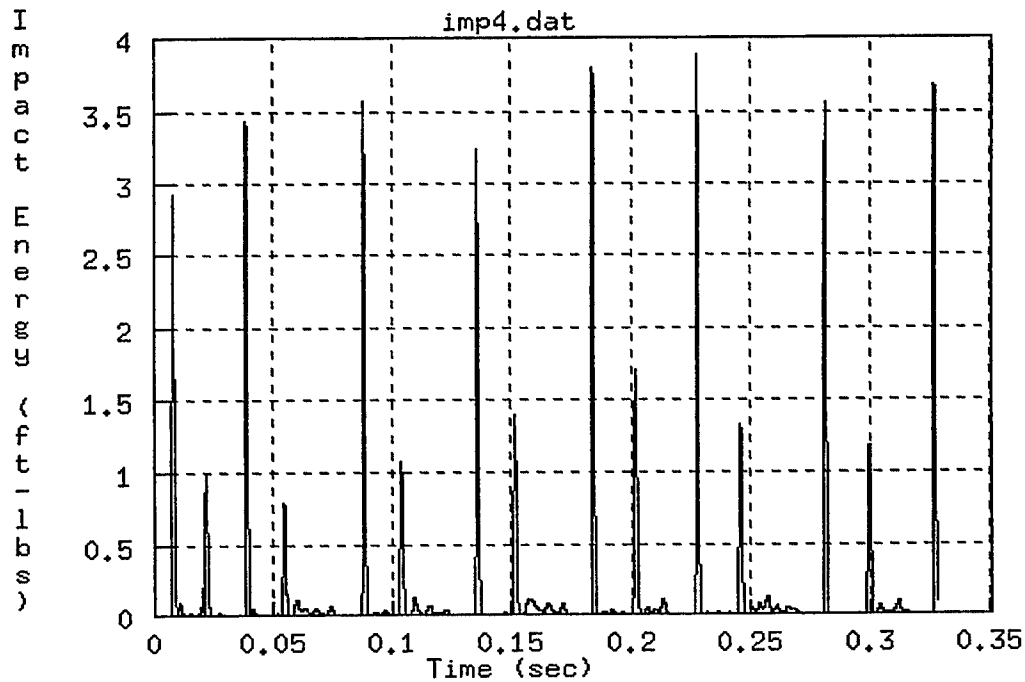
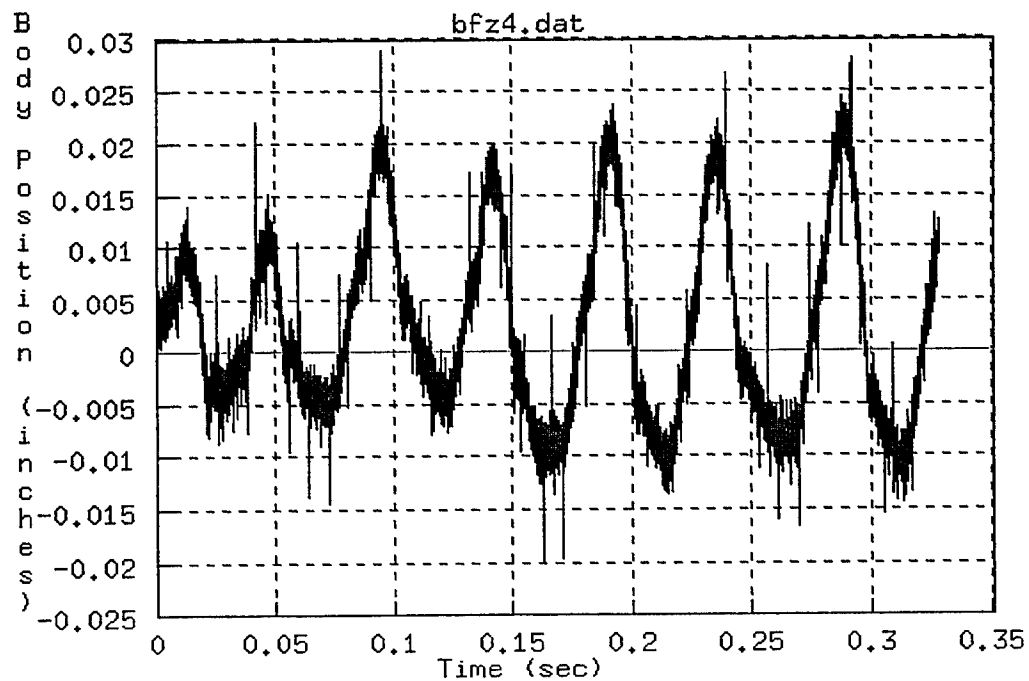


Figure 8
Comparison of drill body displacement for application
of a 100- to 400-pound downward force.

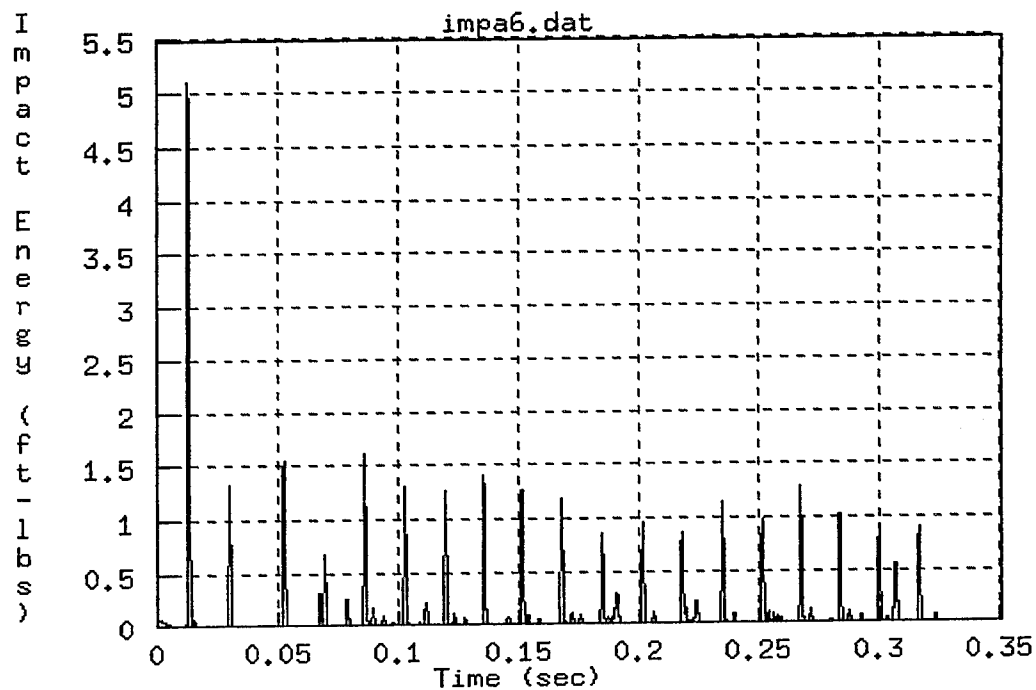


(a) Test 5 impact energy; 1,000 psi, redesigned piston.

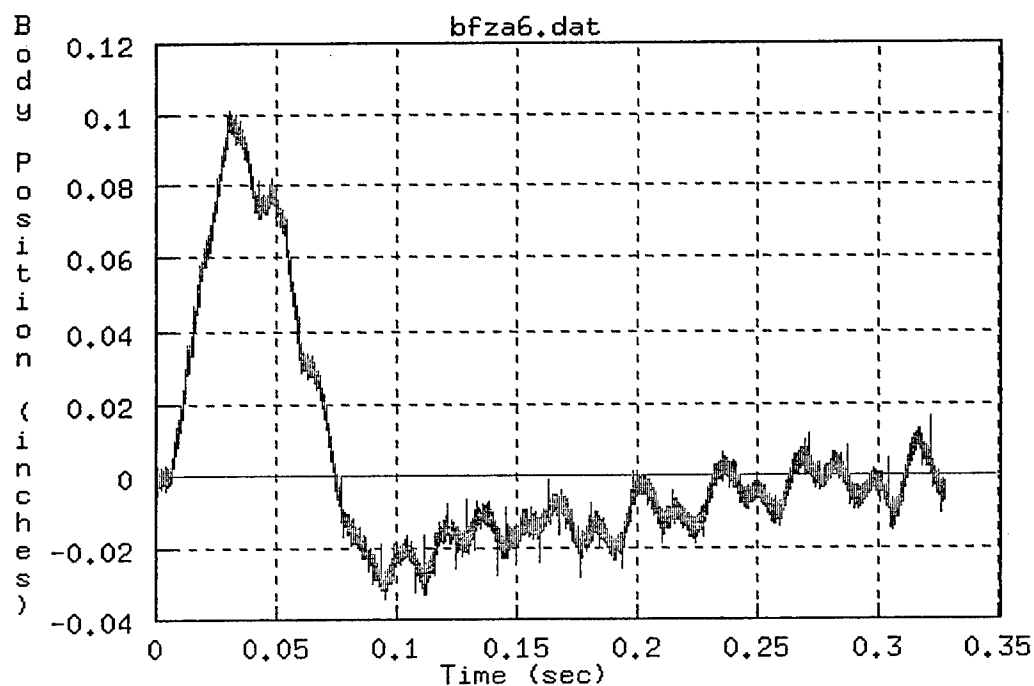


(b) Test 5 body motion; 1,000 psi, redesigned piston.

Figure 9
Test 5 data showing double impact.



(a) Test A6 impact energy; 1,350 psi, redesigned plunger and piston.



(b) Test A6 body motion; 1,350 psi, redesigned plunger and piston.

Figure 10
Drill body displacement and impact energy for second mode operation.

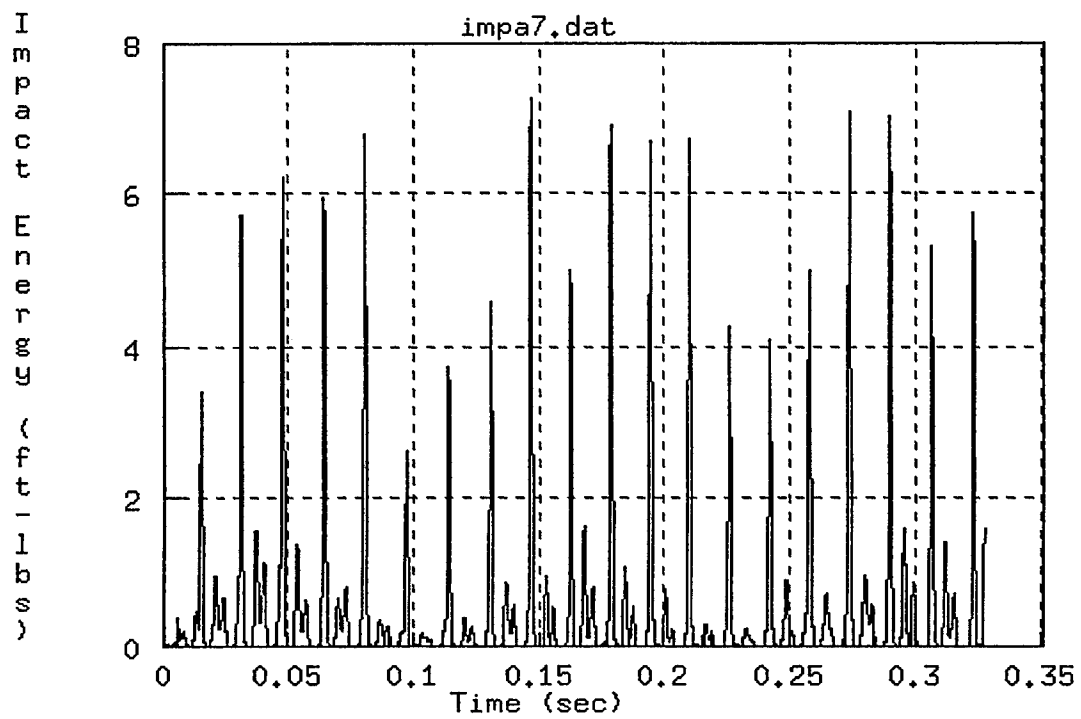


Figure 11
Test A7: nearly half of the impacts were at 6 ft-lb or greater.

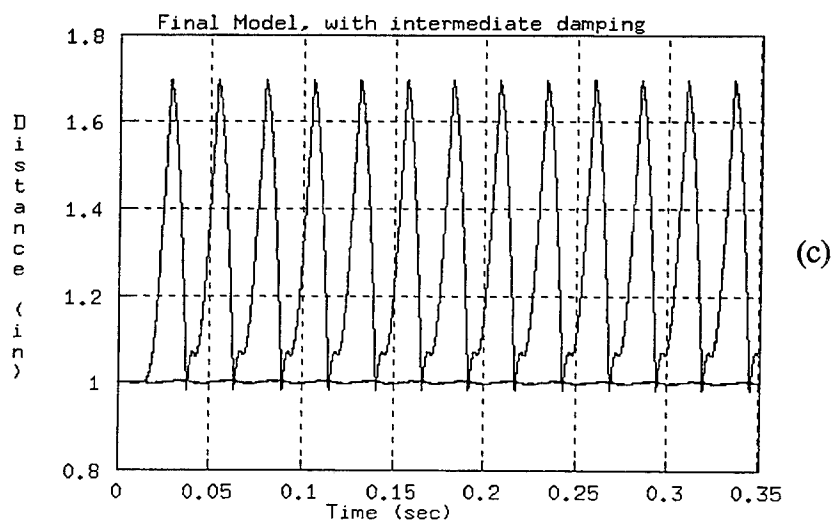
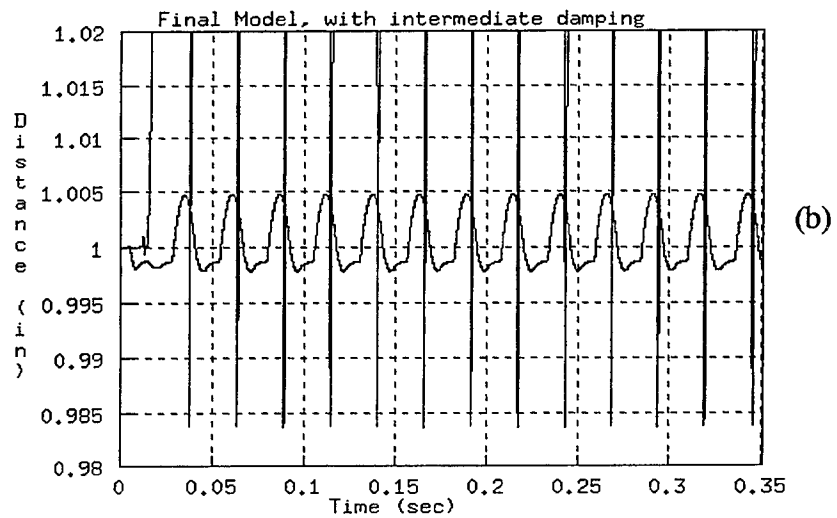
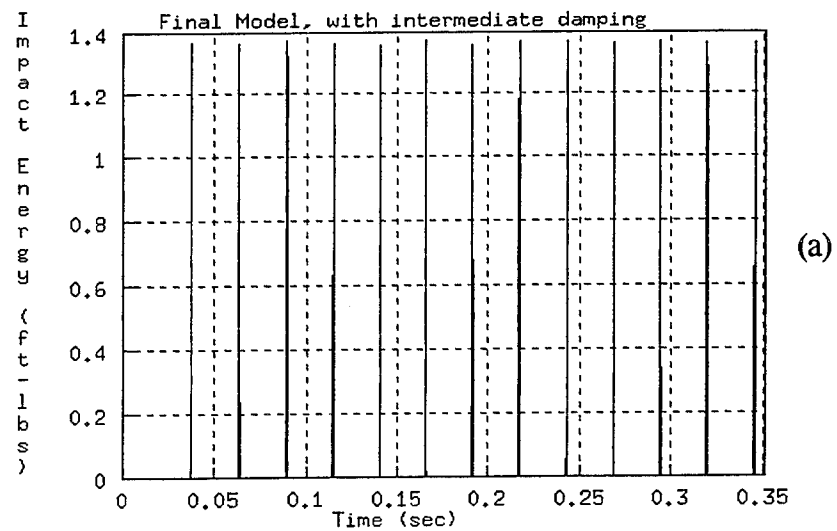


Figure 12
Impact energy (a), body motion (b), and piston stroke (c) relative motion plots for the model with 30 percent damping coefficients.

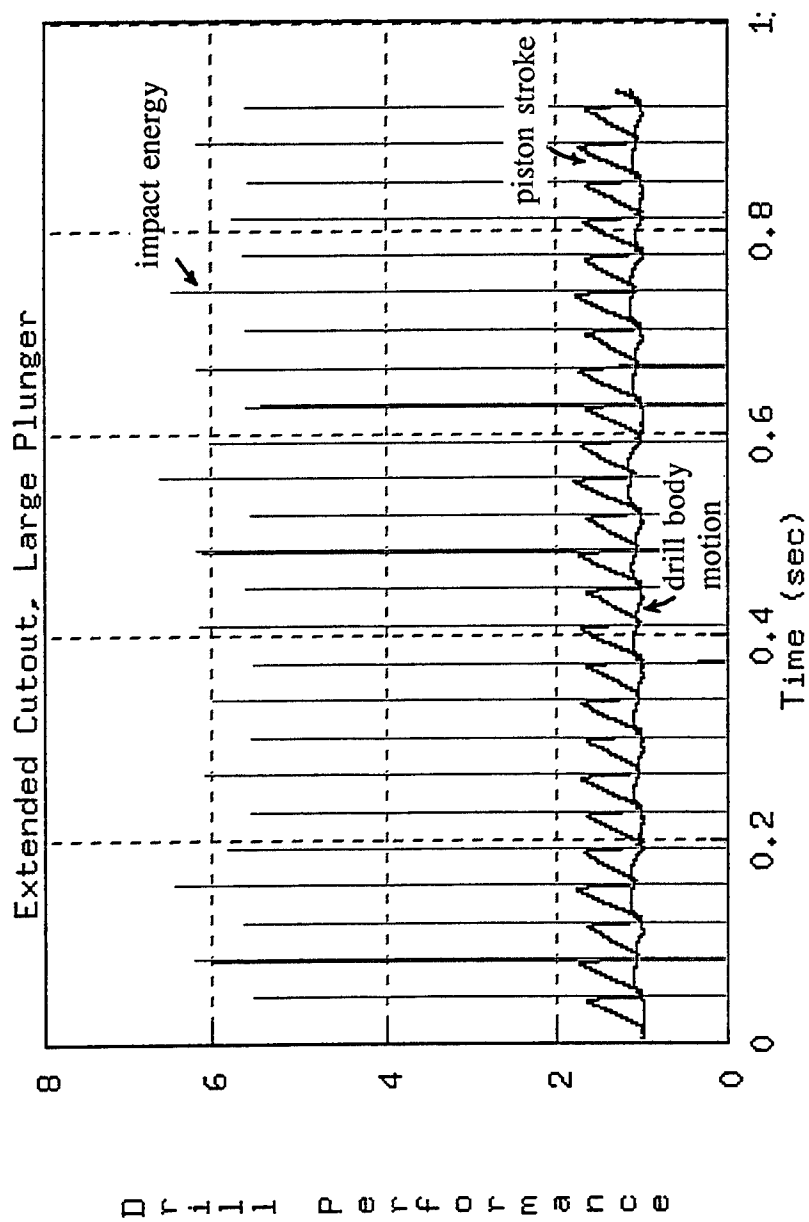


Figure 13
Impact energy, body motion, and piston stroke relative motion plots for
the model with the doubled plunger area.

Appendix A

DETAILS OF DADS MODEL

DYNAMIC MODEL

The software selected for model development was the Dynamic Analysis and Design System (DADS). The developed computer model of the linear impact mechanism qualitatively mimicked empirical test results obtained during prior rock drill evaluation testing. After model validation, parametric studies were performed for comparison to baseline model results. Model refinements lead to predictions of performance improvements.

The basic building blocks for the model consisted of bodies, some fixed to an inertial reference frame, and some allowed to move; joints between the bodies; springs; hydraulic accumulators; valves; actuators; line elements; and control functions. The control and hydraulic functions in the model were divided into four sections:

- 1 - Supply Pressure Activation
- 2 - Poppet Motion
- 3 - Plunger Motion
- 4 - Piston Motion

Figure A-1 shows the activation of the supply pressure. The nominal supply pressure is supplied by a large accumulator (SOURCE). The switch (VALVE.SWITCH) is initially closed and, at a selected time, is opened to supply pressure to the drill (PS).

Figure A-2 shows the effects of poppet motion. The poppet is considered to act as a valve (VALVE.POPPET) which controls flow to the drive chamber. A curve is used to translate the displacement of the poppet (DIS.PPHPO1) into a spool setting (SPOOL.POPPET). In the closed position, the supply pressure applies a force on the poppet (ACT.POPPET1). In addition to the supply pressure acting to open the poppet, the kicker port pressure (PK) acts to hold the poppet closed (ACT.POPPET2). Included is a small biasing spring that works to close the poppet when the pressures are balanced.

When the poppet opens, additional area on the poppet is exposed, and the supply pressure must be applied to the added area. This was initially modeled using a curve to represent the added area and multiplying by the supply pressure to obtain the added force. This was later changed to better reflect a more complex pressure distribution due to the fluid flow velocity decreasing as the flow cross-sectional area increases. A closer approximation was achieved by applying the pressure in the poppet chamber to the added area at all times. This change was made by adding line element (LINE3) discussed below. Poppet chamber pressure (PPO) is applied to the added area to hold the poppet open (ACT.POPPET3).

Figure A-3 shows the operation of the plunger. Flow from the supply port to the kicker port, and from the kicker port to exhaust, is regulated by the position of the plunger. Curves used to represent the plunger as a spool valve were based on the dimensions of the plunger cutout and galleries in the plunger sleeve. These curves are used to translate the displacement of the

plunger (DIS.PPHPL2) into spool settings (SPOOL.PLUNGER.S and SPOOL.PLUNGER.E) for valves controlling flow into and out of the kicker port (VALVE.PLUNGER.S and VALVE.PLUNGER.E, respectively).

Leakage from the kicker port to exhaust was modeled by a small non-zero offset in the exhaust curve (CURVE.PLUNGER.E) leaving the exhaust valve partially open at all times. A similar offset in the supply curve (CURVE.PLUNGER.S) provided for supply leakage. Leakage values of 2 percent for the supply and exhaust side of the plunger were determined to yield a truer match to empirical data. However, the model was extremely sensitive to changes in this parameter.

Line element (LINE2) represents fluid passage between the supply and the kicker port. An additional line element (LINE3) was added between the poppet chamber and the plunger drive chamber to provide information on the pressure drop and flow across the supply poppet, and thus the pressure in the poppet chamber (PPO). The line element (LINE4) added between the plunger drive chamber and the exhaust orifice allowed for a more accurate exhaust behavior and produced a desired lag to the drive chamber discharge. This element provided information on the pressure drop and flow to the exhaust orifice, and thus the pressure in the exhaust chamber (PEY). Later, a line element (LINE5) was added between the plunger and the kicker port on the supply side. This line element served to reduce pressure pulsation in the kicker port to match empirical data.

The drive chamber pressure (PPL), which is a function of the poppet setting, is continuously exhausted through an open orifice (VALVE.EXHAUST). The exhaust condition is represented by a near-infinite volume accumulator (EXHAUST) at ambient pressure (PEY). The drive chamber pressure is applied to the plunger through an actuator (ACT.PLUNGER), and a small force is created by the exhaust pressure acting on the back side of the plunger head (PFORCE.PL).

Figure A-4 shows the working of the piston. The line element (LINE1) represents the fluid between the supply and the piston chamber. The pressure in the piston chamber (PPI) is applied to the differential piston area (ACT.PISTON). The force from this actuator (ACT.FORCE.PISTON), which is calculated as a by-product of the element, is multiplied by a fraction, then applied as a seal friction force (FFORCE.PI). The sign of the piston velocity (DISD.PHPI1) is used to set the sign of the friction force to oppose motion.

Motion of the poppet, plunger, piston, and anvil was limited by hard stops at the upper and lower limits of body motion from housing contact. Hard contacts were also implemented at the interfaces for plunger to piston, and piston to anvil. These hard contacts were implemented through a set of control elements which created a compression only spring damper force. A typical hard-stop control element diagram is shown in Figure A-5. The string labeled "XY" represents the names for the two bodies such as "PLPI" for plunger to piston contact. The displacement (DIS.XY) causes a force (F) to be applied between the two bodies only for values less than zero. The damping coefficient is a function of velocity (DISD.XY).

The coordinate system locations for the noncentroidal reference frames and centers of gravity for the redesign model are shown in Figure A-6. Figure A-7 shows the locations for the hard stops as they were modeled.

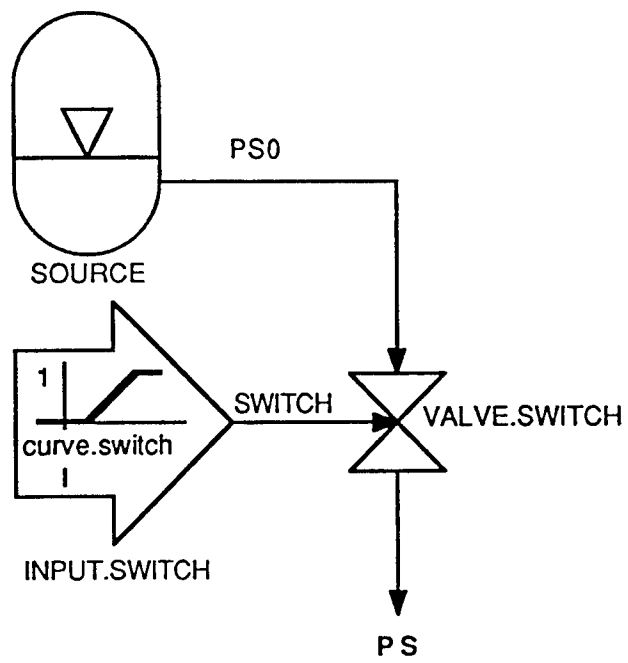


Figure A-1
Supply pressure flow chart for model.

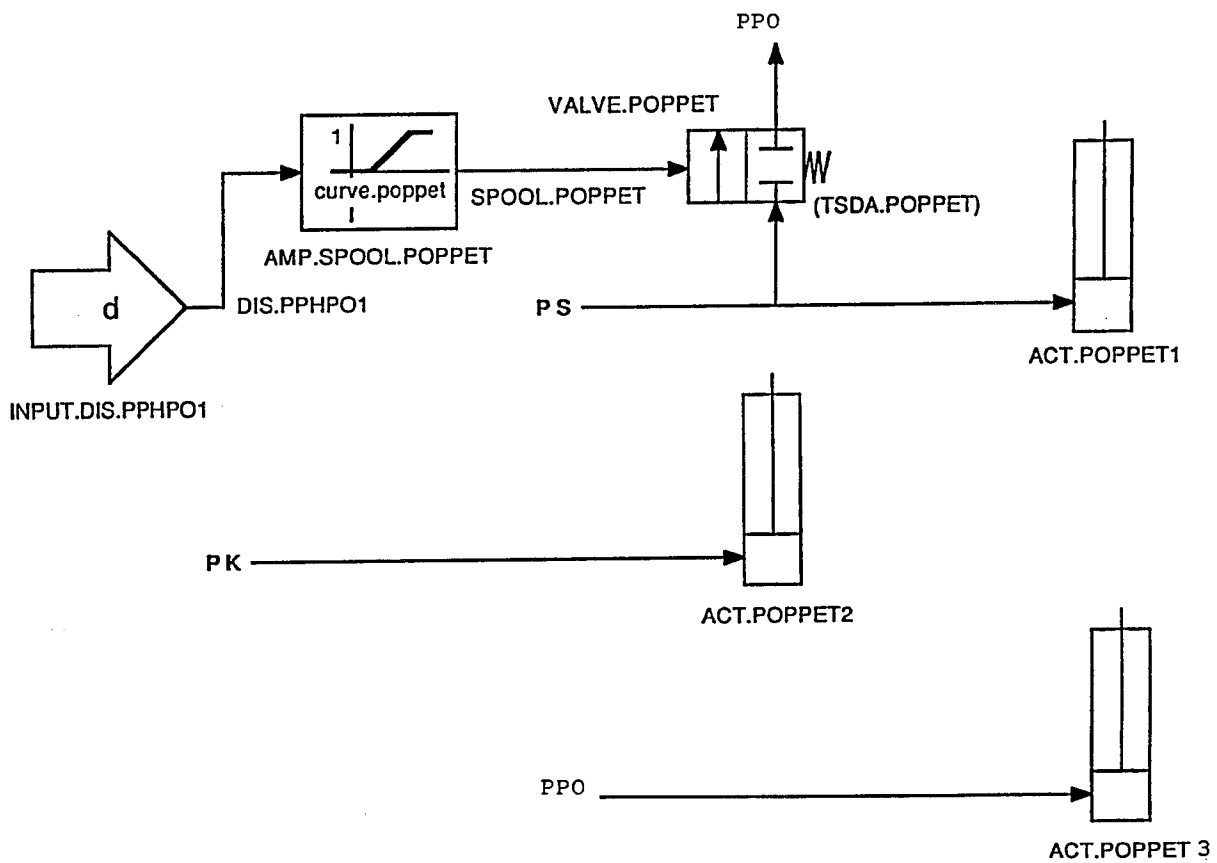


Figure A-2
Supply poppet flow chart for model.

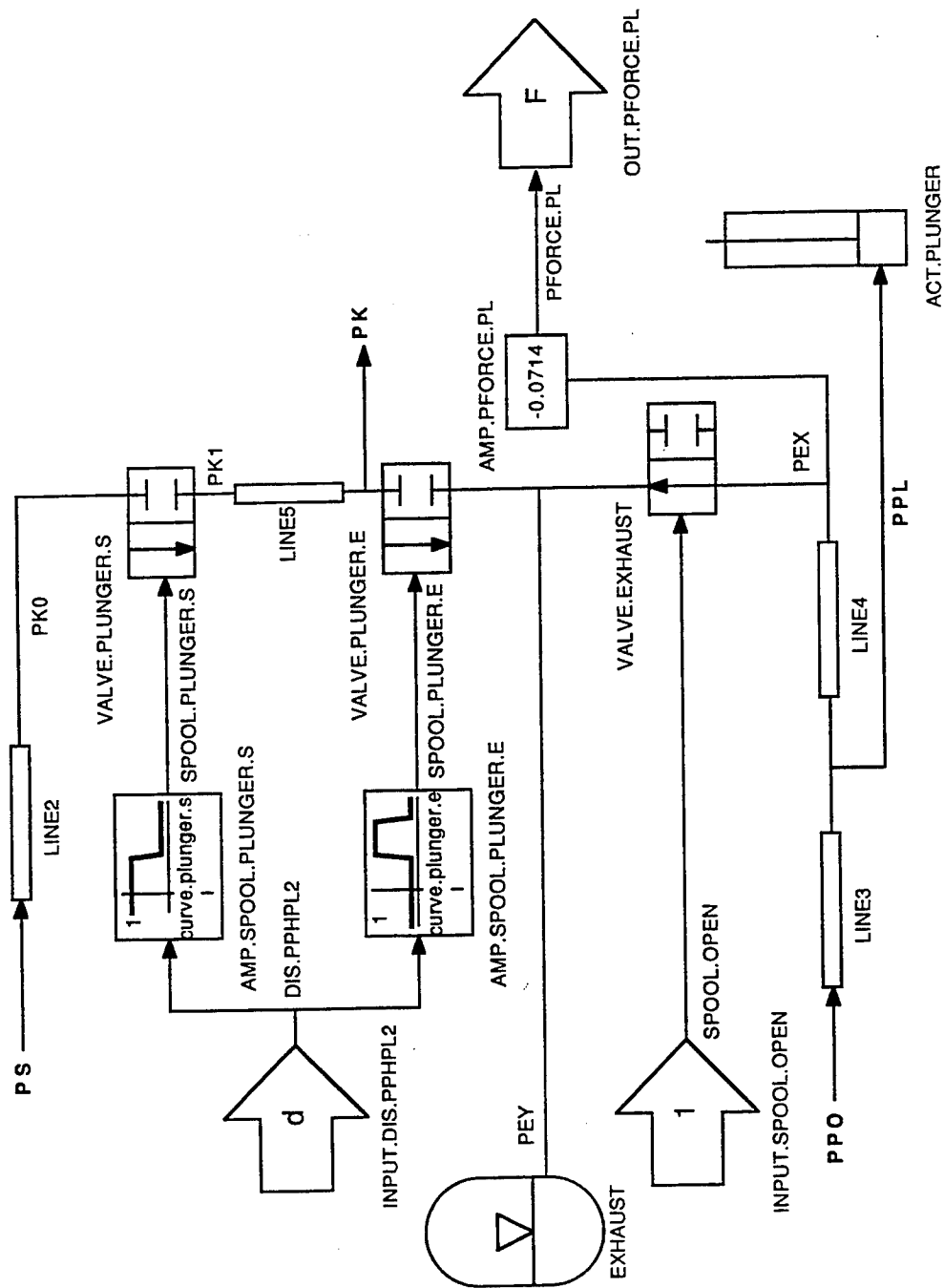


Figure A-3
Plunger flow chart for model.

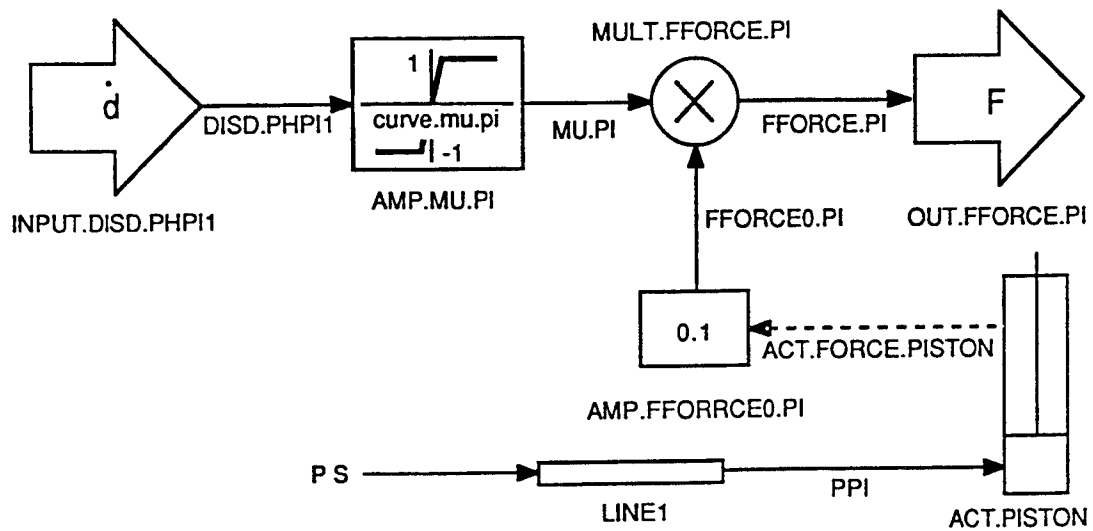


Figure A-4
Piston flow chart for model.

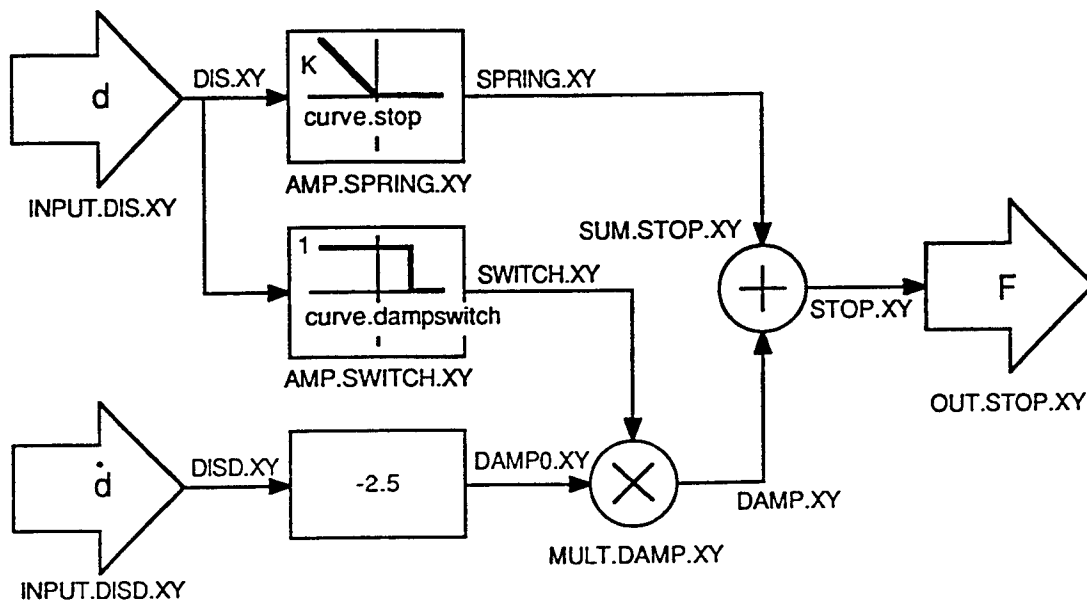


Figure A-5
Sample of hard stop control flow chart.

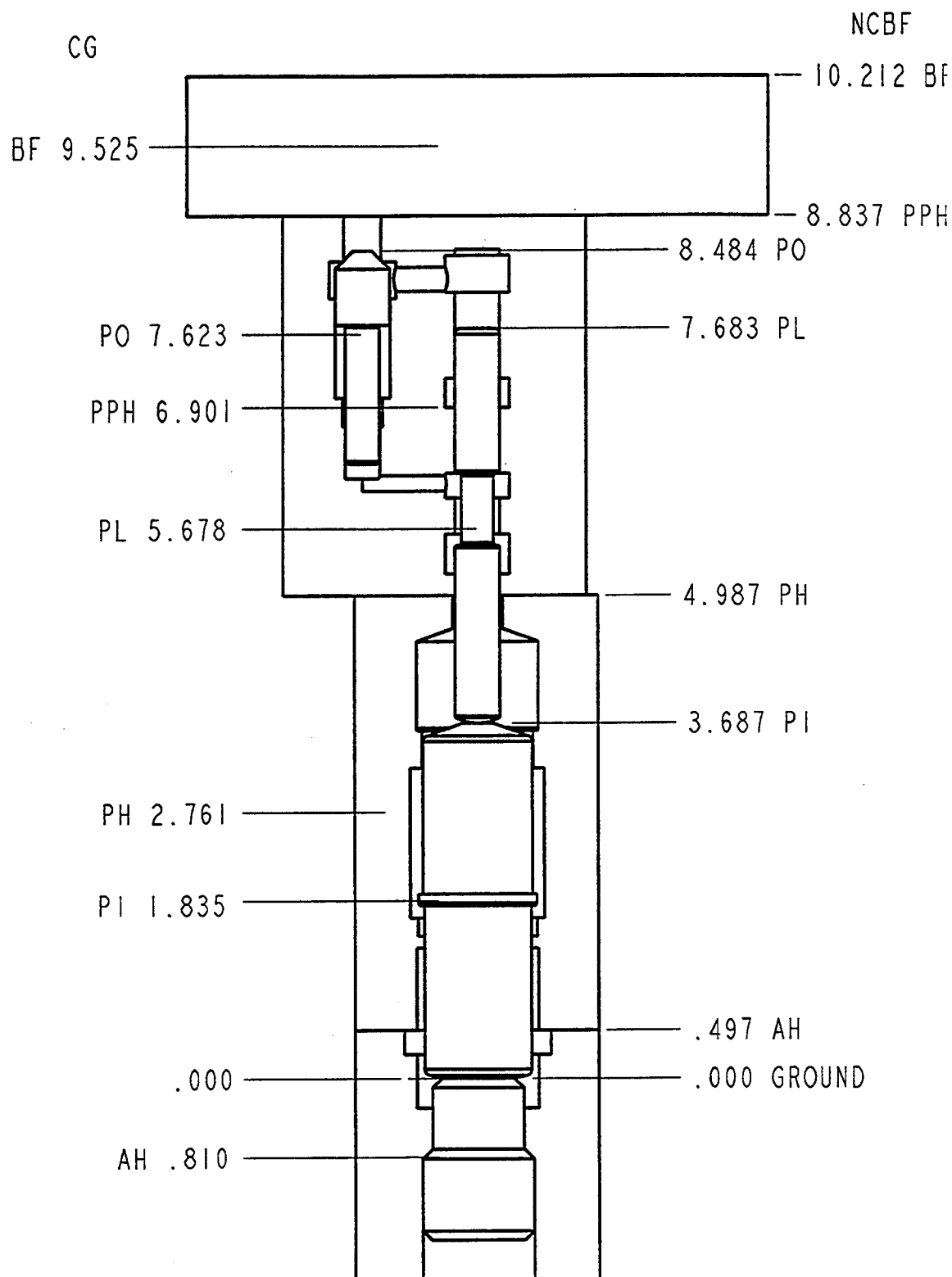


Figure A-6
Coordinate system locations for the noncentroidal reference frames
and centers of gravity for the redesign model.

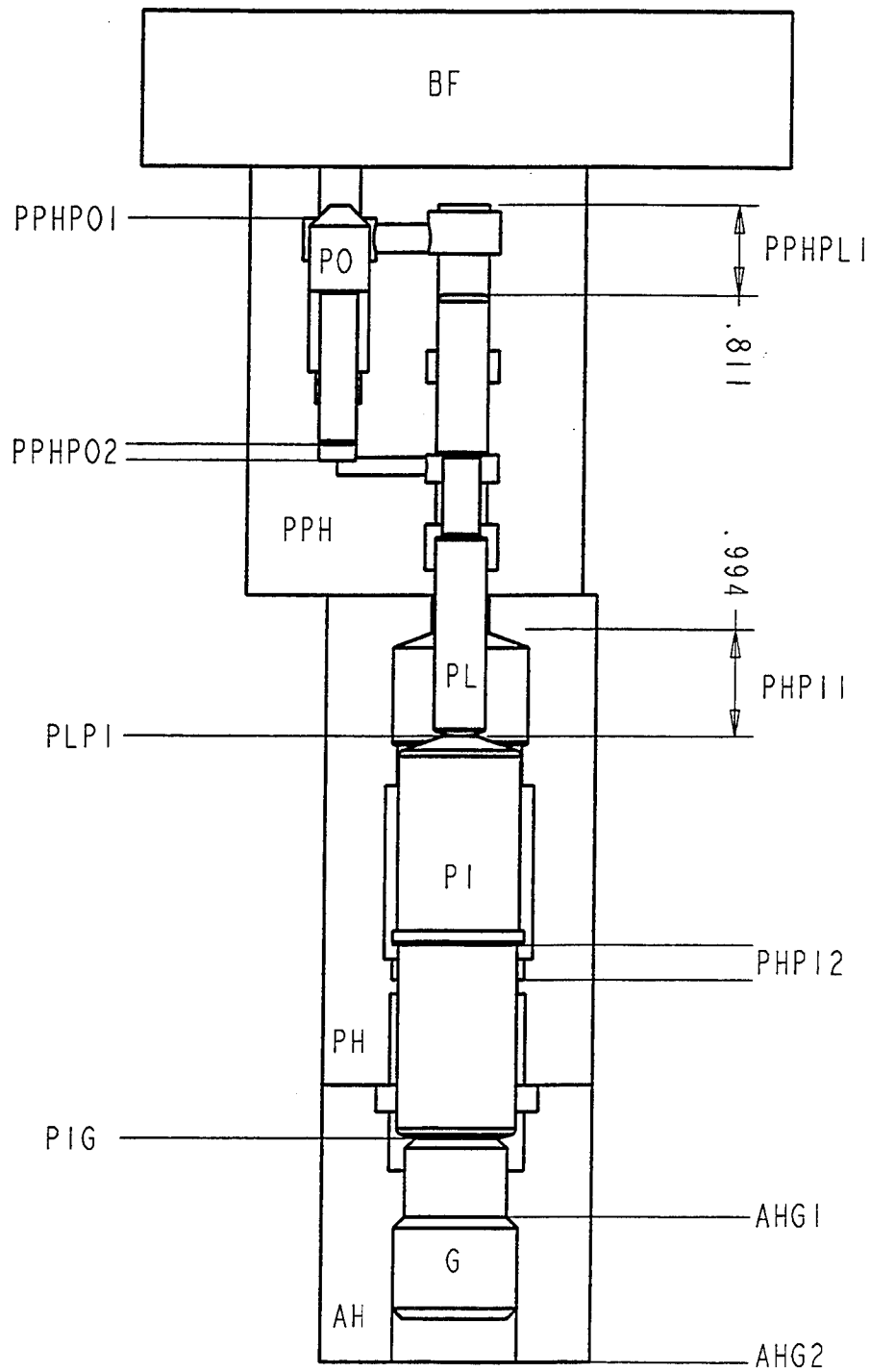
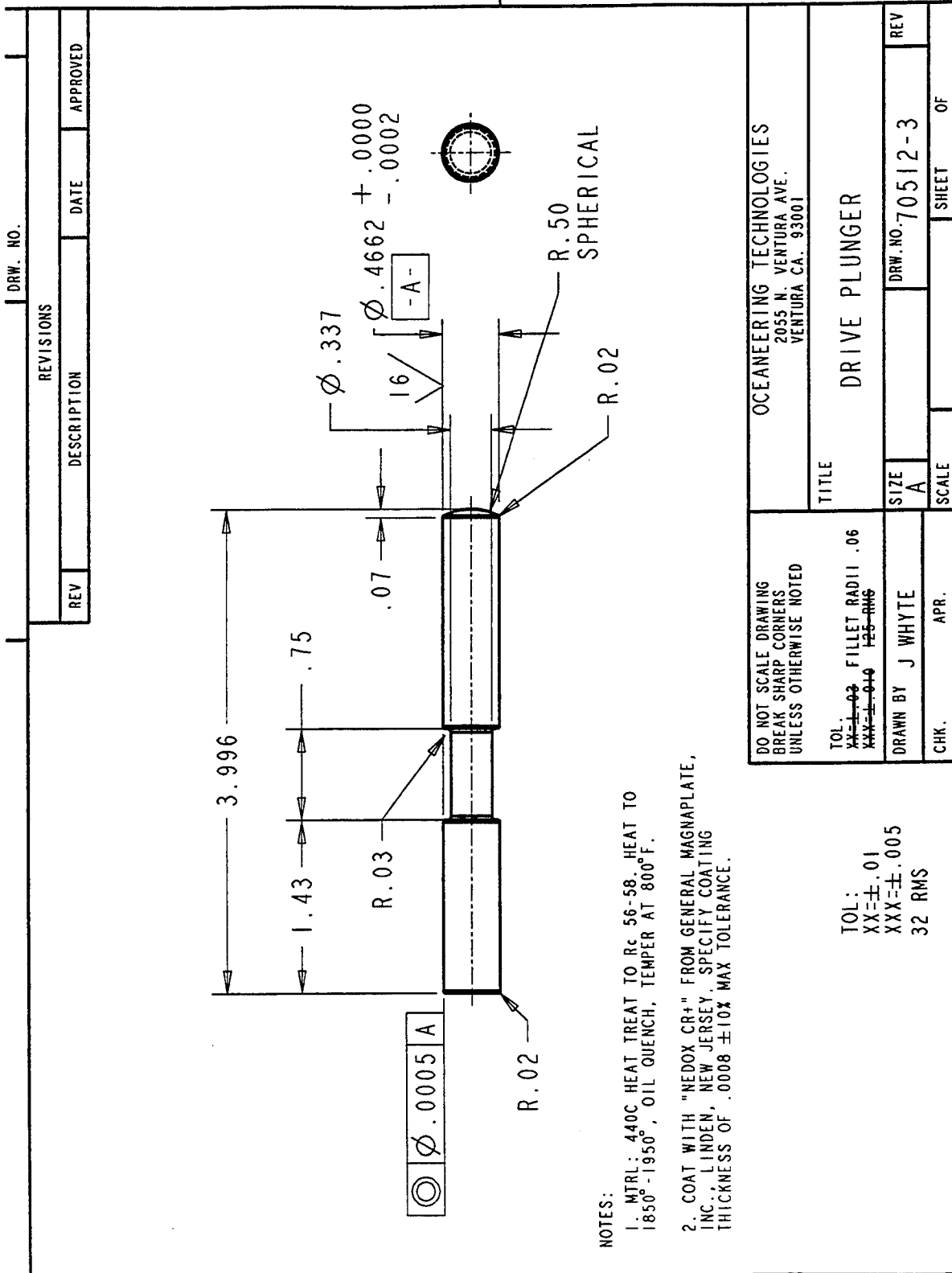
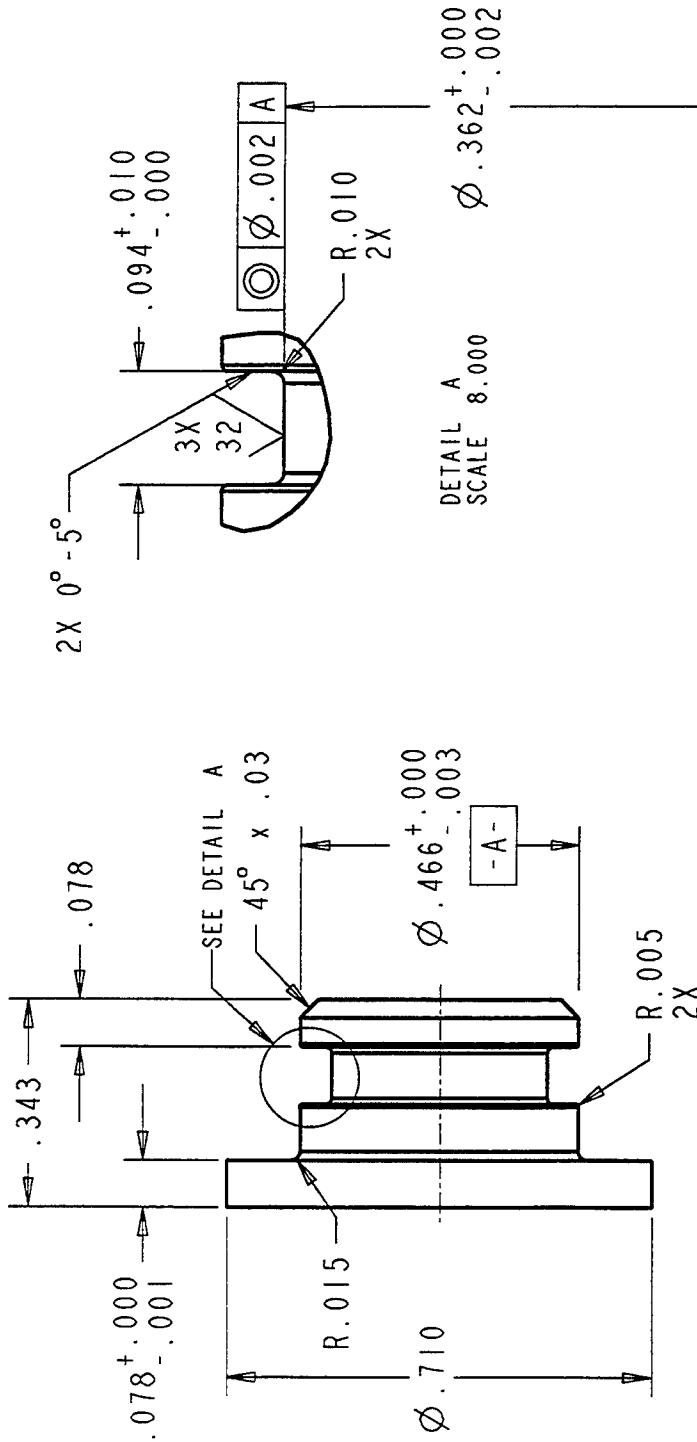


Figure A-7
Locations for the hard stops as they were modeled for the redesign model.

Appendix B
IMPACT MECHANISM PARTS DRAWINGS



REV. NO.		
REVISIONS		
REV	DESCRIPTION	DATE
APPROVED		



NOTES:

1. MATRL: 316 CRES
2. DIAMETERS TO BE U.O.S.
3. TOL. XX=.01
XXX=.005

DO NOT SCALE DRAWING BREAK SHARP CORNERS UNLESS OTHERWISE NOTED		OCEANEERING TECHNOLOGIES 2055 N. VENTURA AVE. VENTURA CA. 93001	
TOL. XX=.01 XXX=.01 Fillet Radii .06 125 RMS		TITLE PLUNGER SLEEVECAP	
DRAWN BY	J WHYTE	SIZE	A
CHK.	APR.	SCALE	4X
		DRW. NO.	70512-4
		SHEET	OF

DISTRIBUTION LIST

AF / ROBERTS, TALLAHASSEE, FL
APPLIED TECHNOLOGY AND MANAGEMENT / C. JONES, CHARLESTON, SC
ARMY CEWES / (TW RICHARDSON), VICKSBURG, MS
ARMY EWES / PERRY, VICKSBURG, MS; WESCD-P (MELBY), VICKSBURG, MS; WESCV-Z
(WHALIN), VICKSBURG, MS
ARVID GRANT & ASSOC / OLYMPIA, WA
BATTELLE / D. FRINK, COLUMBUS, OH; D. HACKMAN, COLUMBUS, OH
BECHTEL CIVIL, INC / K. MARK, SAN FRANCISCO, CA
BING YEN AND ASSOCIATES, INC / IRVINE, CA
BLAYLOCK ENGINEERING GROUP / T SPENCER, SAN DIEGO, CA
BUREAU OF RECLAMATION / D-1512 (GS DEPUY), DENVER, CO; SMOAK, DENVER, CO
CAL STATE UNIV / C.V. CHELAPATI, LONG BEACH, CA
CHAO, JC / HOUSTON, TX
CHEE, WINSTON / GRETN, LA
CHESNAVACENGCOM / CODE FPO-1C, WASHINGTON, DC; LOWER, WASHINGTON, DC
CHILDS ENGRG CORP / K.M. CHILDS, JR., MEDFIELD, MA
CITY OF MONTEREY / CONST MGR (REICHMUTH), MONTEREY, CA
COLLINS ENGRG, INC / M GARLICH, CHICAGO, IL
COLORADO SCHOOL OF MINES / CHUNG,
COLUMBIA GULF TRANSMISSION CO / ENGRG LIB, HOUSTON, TX
COMNAVACT / PWO, LONDON, UK, FPO AE,
COMNAVIAIRSYSCOM / CODE 422, WASHINGTON, DC
COMNAVSURF / CODE N42A, NORFOLK, VA; LANT, CO, NORFOLK, VA; PAC, CODE N-4,
SAN DIEGO, CA
COMSUBDEVGRU ONE / OPS OFFR, SAN DIEGO, CA
CONSTRUCTION TECH LABS, INC / G. CORLEY, SKOKIE, IL
CORNELL UNIV / CIVIL & ENVIRON ENGRG, ITHACA, NY
DCD, USAES / ATSE-CDM-S (SFC FARBER), FT LEONARD WOOD, MO
DEPT OF BOATING / ARMSTRONG, SACRAMENTO, CA
DFSC-F / ALEXANDRIA, VA
DTRC / CODE 2724, BLOOMQUIST, ANNAPOLIS, MD
EODMU THREE / CODE 3265, POINT MUGU, CA
EXXON PRODUCTION RSCH CO / OFFSHORE OP DIV, HOUSTON, TX
GEOCON INC / CORLEY, SAN DIEGO, CA
GRUMMAN AEROSPACE CORP / TECH INFO CENTER, BETHPAGE, NY
HALEY & ALDRICH, INC. / CETIN SOYDEMIR, CAMBRIDGE, MA
HAN-PADRON ASSOCIATES / DENNIS PADRON, NEW YORK, NY
HARDY, S.P. / SAN RAMON, CA
HARTER, J.V. / METAIRIE, LA
HERONEMUS, W.E. / AMHERST, MA
INTL MARITIME, INC / D. WALSH, MYRTLE POINT, OR
IOWA STATE UNIV / CE DEPT, AMES, IA
LANDAU ASSOC / STIRLING, EDMONDS, WA
LONG BEACH PORT / ENGRG DIR (ALLEN), LONG BEACH, CA; ENGRG DIR (LUZZI),
LONG BEACH, CA
MARATHON OIL CO / GAMBLE, HOUSTON, TX
MARITECH ENGRG / DONOGHUE, AUSTIN, TX
MBARI / SHANE, MOSS LANDING, CA

MC CLELLAND ENGRS, INC / LIB, HOUSTON, TX
 MC DERMOTT, INC / E&M DIV, NEW ORLEANS, LA
 MCAS / 16, MAG, TUSTIN, CA; PWO, KANEOHE BAY, HI
 MCRD / PWO, SAN DIEGO, CA
 MICHIGAN TECH UNIV / CO DEPT (HAAS), HOUGHTON, MI
 MOBIL R&D CORP / OFFSHORE ENGRG LIB, DALLAS, TX
 MT DAVISSON / CE, SAVOY, IL
 NAVAIRWPNSTA / CODE P3614 (NUSSEAR), POINT MUGU, CA
 NAVCOASTSYSCEN / PWO (CODE 740), PANAMA CITY, FL
 NAVCONSTRACEN / PLATT, PORT HUENEME, CA
 NAVDIVESALVTRACEN / CO, PANAMA CITY, FL
 NAVFACENGCOM / CODE 04A3C, HUBLER, ALEXANDRIA, VA; CODE 1232F (LT WEIL),
 ALEXANDRIA, VA
 NAVOCEANO / CODE 6200 (M PAIGE), NSTL, MS
 NAVSHIPYD / CARR INLET ACOUSTIC RANGE, BREMERTON, WA
 NAVSPNSTA / PWO, CHARLESTON, SC
 NAVSTA / ENGR DIV, PWD, FPO AA; PWO, ROTA, SPAIN, FPO AE
 NAVSTA PUGET SOUND / CODE 922, EVERETT, WA
 NAVSUPACT / CODE 430, NEW ORLEANS, LA
 NAVSUPPFAC / CONTRACT ASSISTANT, FPO AP
 NCCOSC / DIV 9407, SAN DIEGO, CA; ROBERT WERNLI, SAN DIEGO, CA
 NOAA / JOSEPH VADUS, ROCKVILLE, MD
 NORDA / CODE 500, NSTL, MS
 NORTHDIV CONTRACTS OFFICE / ROICC, PORTSMOUTH, NH
 NSF / (N32), NORFOLK, VA
 NUSC / CODE 0031 DIVING OFFR, NEWPORT, RI
 NUSC DET / NEWPORT, RI; CODE 2143 (VARLEY), NEW LONDON, CT; CODE TA131,
 NEW LONDON, CT; DOC LIB, NEW LONDON, CT
 OCEANEERING TECH / VENTURA, CA
 OCNR / CODE 1121 (EA SILVA), ARLINGTON, VA
 OMEGA MARINE, INC. / SCHULZE, LIBRARIAN, HOUSTON, TX
 PACIFIC MARINE TECH / M. WAGNER, DUVALL, WA
 PACNAVFACENGCOM / CODE 102, PEARL HARBOR, HI
 PURDUE UNIV / CE SCOL (ALTSCHAEFFL), WEST LAFAYETTE, IN; CE SCOL (LEONARDS),
 WEST LAFAYETTE, IN; ENGRG LIB, WEST LAFAYETTE, IN
 PWC / CODE 421 (KAYA), PEARL HARBOR, HI; CODE 421 (QUIN), SAN DIEGO, CA
 Q ASSOCIATES / QUIRK, J PANAMA CITY, FL
 R J BROWN & ASSOC / R PERERA, HOUSTON, TX
 SAN DIEGO PORT / AUSTIN, SAN DIEGO, CA
 SAN DIEGO STATE UNIV / CE DEPT (NOORANY), SAN DIEGO, CA
 SCHUPACK SUAREZ ENGRS INC. / SCHUPACK, NORWALK, CT
 SEAL TEAM / 6, NORFOLK, VA
 SEATTLE UNIV / CE DEPT (SCHWAEGLER), SEATTLE, WA
 SOUTHWEST RSCH INST / KING, SAN ANTONIO, TX
 T.C. DUNN / SHREWSBURY, MA
 TEXAS A&M UNIV / CE DEPT (HERBICH), COLLEGE STATION, TX; OCEAN ENGR PROJ,
 COLLEGE STATION, TX
 TWELVE OAKS BUSINESS PARK / WEST HAVEN, CT
 UNIV OF CALIFORNIA / CE DEPT (MITCHELL), BERKELEY, CA; NAVAL ARCHT DEPT,
 BERKELEY, CA
 UNIV OF HAWAII / LOOK LAB, OCEAN ENGRG, HONOLULU, HI; MANOA, LIB, HONOLULU, HI;
 OCEAN ENGRG DEPT (ERTEKIN), HONOLULU, HI
 UNIV OF MICHIGAN / CE DEPT (RICHART), ANN ARBOR, MI
 UNIV OF NEW HAMPSHIRE / LAVOIE, DURHAM, NH

UNIV OF RHODE ISLAND / PELL MARINE SCI LIB, NARRAGANSETT, RI
UNIV OF TEXAS / CONSTRUCTION INDUSTRY INST, AUSTIN, TX
UNIV OF WISCONSIN / GREAT LAKES STUDIES CEN, MILWAUKEE, WI
USACOE / CESPDCO-EQ, SAN FRANCISCO, CA
USAE / CEWES-IM-MI-R, VICKSBURG, MS
USDA / FOR SVC, EQUIP DEV CEN, SAN DIMAS, CA
USN / CAPT COLIN M JONES, HONOLULU, HI
USNA / OCEAN ENGRG DEPT, ANNAPOLIS, MD
VSE / OCEAN ENGRG GROUP (CHASE), ALEXANDRIA, VA
WESCR-P / HALES, VICKSBURG, MS
WESTNAVFACENGCOM / CODE 407, SAN BRUNO, CA; ROICC, SILVERDALE, WA
WISWELL, INC. / SOUTHPORT, CT
WOODS HOLE OCEANOGRAPHIC INST / DOC LIB, WOODS HOLE, MA
WOODWARD-CLYDE CONSULTANTS / R. CROSS, OAKLAND, CA; WEST REG, LIB, OAKLAND, CA